Estimation of Frequency Control Performance Using Probability Distribution of Load Change

by

Thusitha Wickramasinghe

A Thesis submitted to the Faculty of Graduate Studies of
The University of Manitoba
in partial fulfillment of the requirements of the degree of

MASTER OF SCIENCE

Department of Electrical and Computer Engineering
University of Manitoba
Winnipeg, Manitoba

Abstract

In North American utilities, control area performance of interconnected power systems is assessed by the reliability standards imposed by the North American Electric Reliability Corporation (NERC). NERC standards on control area performance define two indices known as Control Performance Standards 1 and 2 (CPS1 and CPS2) to evaluate control area performance in normal interconnected power system operation. Out of the two indices, CPS1 evaluates the performance of a control area with respect to control of interconnection frequency and tie-line power flows. This thesis proposes a novel method to approximately estimate CPS1 for a two area power system using the probability distribution of load change.

The proposed method of estimating CPS1 is validated against the time domain simulation method using a simple two-area test system. In the validation process, it is shown that the proposed method could approximately forecast CPS1 within 5% accuracy. The forecasted CPS1 value could then be used by a control area to design its future control strategies to be in compliance with NERC criteria at the minimum cost. These control actions include, but not limited to tuning governors, reducing non-confirming loads, ensuring adequate operating and spinning reserves etc.

Acknowledgements

I would like to express my gratitude and appreciation to my thesis advisor, Professor Udaya Annakkage for proposing the thesis topic and for his continuous advice and guidance. The valuable input from Professor R. Karki from University of Saskatchewan is highly appreciated and gratefully acknowledged.

I would like to thank Manitoba Hydro for the partial financial assistance granted for my tuition fees.

I must also thank the technical staff at the Department of Electrical and Computer Engineering, especially Mr. Erwin Dirks for his support. I would like to thank my friends and the staff of the Department of Electrical and Computer Engineering for their continuous encouragement and for making my years at the University of Manitoba a pleasant experience.

This acknowledgement will be incomplete without thanking my husband for his valuable suggestions and encouragement throughout the course of this work. I would also extend my heartfelt gratitude to my parents and two sisters for all the love and support.

Thusitha Wickramasinghe

June 2010

Table of Contents

List of Figures

List of Tables

List of Symbols

CPC	Control Performance Criteria
CPS	Control Performance Standard
CPS1	Control Performance Standard 1
CPS2	Control Performance Standard 2
ACE	Area Control Error
AGC	Automatic Generation Control
CF	Compliance Factor
$CF_{i\text{-}1M}$	Clock-one-minute CF of area i
Δf_i	Frequency error of area i
ΔP_{ij}	Tie-line power flow error in from area i to area j
$\Delta f_{i\text{-}1M}$	Clock-one-minute average value of frequency error in area i
D	Load Damping Constant
R	Speed Regulation or Droop
B_i	Frequency Bias Factor of area i
ε_1	Targeted RMS value of clock-one-minute-average frequency error from schedule
m	Load sampling time
ΔP_L	Load Change

Chapter 1
Introduction

1.1 Background

Electricity is a distinct commodity in which generation and consumption must be matched instantaneously at all times. Unlike other forms of energy, electricity cannot be produced and stored in large quantities in advance for future use; hence a sophisticated control system is required to ensure that the generation meets the continually changing load demand for real and reactive power. Real power control is closely related to frequency control; hence in order to maintain the system frequency at its nominal value, the real power generation should be equal to the real power consumption of the load. Mismatches between the real power produced by the generators and the real power consumed by the load will result in frequency deviations. Frequency deviations up to ±0.5 Hz from the nominal system frequency is considered as normal in North American power system operation [1]. However large frequency deviations could adversely affect the normal power system operation, which could ultimately lead to system collapse. Hence for satisfactory performance of a power system, the frequency should remain nearly at its nominal value. Similarly, reactive power control is closely related to voltage control; hence in order to maintain steady acceptable voltages at all buses, the system should be able to meet the reactive power demand of the load.

In an interconnected power system with two or more independently controlled areas, each control area is responsible to maintain pre-agreed power interchange(s) with the

neighboring control areas. Hence, in an interconnected power system, in addition to the control of frequency and voltage, the generation within each area has to be controlled to maintain scheduled power interchange. The control of generation and frequency is commonly referred to as Load-Frequency Control (LFC) [2]. Therefore, the main objectives of the LFC are to keep the system frequency at the nominal value and to maintain the net inter-area power flows at their pre-agreed contract values. This is essential for reliable and secure operation of an interconnected power system, which in turn is vital to the business of the electric power industry.

The electrical power industry in North America began its large scale operation in the first half of the 20th century [1]. This necessitated the utility companies to deliver power to their customers more effectively and efficiently to gain economies of scale. Hence, the newly formed utility companies created 'power pools' with nearby utility companies. The objective was to operate jointly to schedule generation in a cost-effective manner, which helped to reduce operational costs for all members of the pool. The world's first continuous power pool resembling the modern national grid was formed in 1927, when three companies namely the Public Service Electric and Gas Company, Philadelphia Electric Company and Pennsylvania Power & Light Company, formed the Pennsylvania-New Jersey Interconnection [3]. Since then, the interconnection became geographically larger by connecting a large number of formerly isolated bulk electricity suppliers. Eventually the transmission system of electric utilities in the United States and Canada interconnected into a large power grid, known as the "North American Power Systems Interconnection", consisting of four interconnections [4]: the Eastern Interconnection, the Western

Interconnection, the Electric Reliability Council of Texas (ERCOT) interconnection and the Quebec Interconnection. The Eastern Interconnection is the largest out of four and covers most of Eastern North America, excluding most of Texas. The Western Interconnection, the second largest, covers most of Western North America and has several High Voltage Direct Current (HVDC) connections to the Eastern Interconnection. The ERCOT Interconnection covers most of the State of Texas and has an HVDC connection to the Eastern interconnection. Quebec interconnection covers the province of Quebec and operates as a separate interconnection. It has an HVDC interconnection to the Eastern Interconnection.

Figure 1-1, which is extracted from [4] shows the approximate geographical boundaries of the four interconnections mentioned above.

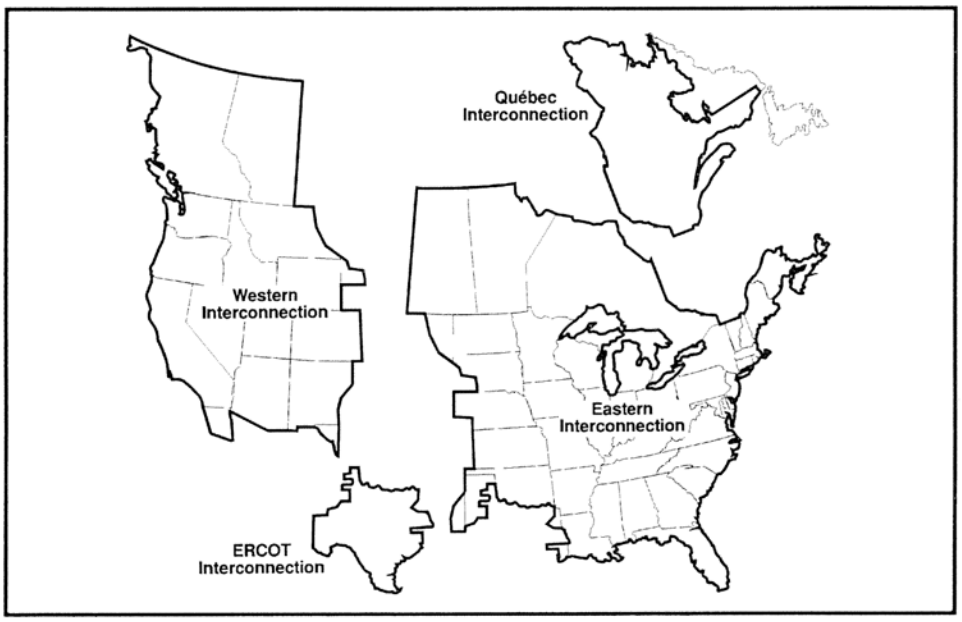

Figure 1-1: Interconnections in North American Electric grid

An interconnection is comprised of "control areas" among which the monitoring and controlling function is decentralized [4]. A control area is connected to other control areas via tie lines. All control areas within an interconnection are synchronized at an average of 60Hz. Therefore, each control area in an interconnection is responsible to maintain its frequency at the nominal value of 60Hz, while continuously controlling its generation to meet the net scheduled interchange. The nominal frequency is also known as the scheduled system frequency and is the frequency that a power system or an interconnected system attempts to maintain [5]. The net scheduled interchange is the net power flow that a control area attempts to maintain on its area tie lines [5].The benefits of interconnected operation should be fairly distributed among all the control areas in an interconnection and should not be unduly exploited by some. For example, if an area is continuously receiving support from a neighboring area to meet its control obligations without supporting any, such an area should be penalized. Hence, there should be a proper mechanism to measure the control area performance of an interconnected power system.

In North American utilities, control area performance has been assessed by the Reliability Standards imposed by the North American Electric Reliability Corporation[1] (NERC) [4]. NERC works with eight regional entities, which are known as Regional Reliability Councils to enforce control areas to comply with its reliability standards. NERC with its regional reliability councils covers all of the interconnected power systems of the United States, Canada and a portion of Baja California in Mexico [6]. Midwest Reliability

[1] North American Electric Reliability Council was formed on June 1st 1968 and became North American Electric Reliability Corporation on March 28th 2006 [6].

Organization (MRO) is one of NERC's regional reliability councils within the Eastern interconnection .The province of Manitoba lies within the jurisdiction of MRO.

1.2 Control Area Performance

In North American utilities, control area performance of an interconnected power system has been assessed by Control Performance Criteria (CPC) imposed by NERC, for several decades [4]. CPC comprised of 4 indices namely A1, A2, B1 and B2 and specified compliance criteria for each one of them. A1 and A2 set the system performance requirements under normal operating conditions whereas B1 and B2 set the system performance requirements under disturbance conditions [7]. In [8], a "disturbance" is defined as

1. An unplanned event that produces an abnormal system condition.
2. Any perturbation to the electric system.
3. The unexpected change in Area Control Error (ACE) that is caused by the sudden failure of generation or interruption of load. ACE is a control signal made up of a control area's tie line power flow deviation from the scheduled value, plus a factor proportional to the area's frequency deviation from the nominal system frequency.

The A1 and A2 criteria are simple and straightforward and relate to an area's ACE. ACE is explained in more detail in Chapter 2. Criterion A1 specified that ACE must return to zero, within 10 minutes of previously reaching zero (i.e. ACE should cross zero at least once

in every 10 minutes) [7],[9]. Criterion A2 specified that the 10-minute average value of ACE should not exceed a certain MW limit known as L_d, which is an area specific parameter determined from the control area's load characteristics [7],[9].

Similarly B1 required that ACE return to zero within 10 minutes following the start of a disturbance whereas B2 required that ACE begin to trend toward zero within one minute following the start of a disturbance [7],[9]. However, it has been pointed out recently that these criteria do not have a sound technical foundation and hence could not be directly used to evaluate reliable control area performance [9]. Four shortcomings of A1 and A2, which made them obsolete in a competitive market-based economy, have been identified in the following list [10].

1. A1 and A2 are based on "mature operating experience and judgment", however they lack theoretical justification to directly relate them to any reliability parameter.
2. A1 and A2 do not provide a direct measure of the impact of ACE on the interconnection. With A1 and A2, all excursions are treated equally regardless of magnitude.
3. A1 and A2 are blind to the fact that ACE can be in a direction to support the interconnection frequency. A1 and A2 will require control actions to correct ACE, even if the ACE assists the frequency. At times, ACE may be moved in a direction that pushes frequency further off schedule.

4. Control areas make a considerable attempt to meet A1 and A2 criteria, which are often costly. It is increasingly more difficult to justify those expenses when A1 and A2 have no solid theoretical justification.

As a result, North American Electric Reliability Council (NERC) replaced the Control Performance Criteria with two new standards namely Control Performance Standard (CPS) and Disturbance Control Standard (DCS), on February 1, 1997 [9].

CPS is comprised of two indices known as Control Performance Standard 1 (CPS1) and Control Performance Standard 2 (CPS2) which replaced criteria A1 and A2 respectively [9]. DCS replaces B1 criterion whereas B2 criterion is no longer required in the new DCS [7].

CPS1 sets a limit on the average of a function which comprises of ACE and interconnection frequency error [9]. Frequency error is the difference between the actual interconnection frequency and its scheduled value [8]. CPS2 limits the magnitude of ten-minute average value of ACE [9]. Thus CPS2 is similar to A2, but the specification for the limit on the ten-minute average ACE value is argued to be technically defensible [9].

According to NERC standards, each control area is expected to be no less than 100% in compliance with CPS1 and 90% in compliance with CPS2 [9]. NERC Regional Reliability Councils are responsible for monitoring compliance of the registered control areas within their regional boundaries, assessing penalties and sanctions for areas failing to comply with the standards [6].

1.3 Control Performance Standard

When compared with A1 and A2, CPS1 and CPS2 are claimed to be better indicators in measuring control area performance. The following list summarizes the merits of CPS over A1 and A2 [7], [9], [10], [11].

1. CPS has a technically defensible basis, developed from mathematical relations between interconnection ACEs and frequency error.
2. CPS can be applied fairly to all types of areas irrespective of their size or other system parameters.
3. CPS demands less unit maneuvering, which results in significant savings in fuel costs and unit wear and tear. This is realized due to the elimination of the ACE zero crossing requirement, which effectively helps to reduce the number of control actions deployed by the area.
4. CPS is capable of evaluating both primary and secondary controls (which are explained in detail in Chapter 2) deployed in a power system to maintain load and generation in balance. ACE, which is the basis of A1 and A2, on the other hand, cannot always evaluate primary controls.

This thesis focuses on CPS1 and details of its definition and calculation procedure is explained in Chapter 3.

1.4 Motivation Behind the Research

CPS1 for each area is estimated using the recorded values of area frequency deviations and deviations of inter-area power flows during the actual system operation [4].

On the other hand, when the load forecast is available, values of area frequency deviations and deviations of inter-area power flows have to be estimated using time domain simulation to estimate CPS1 values for the period of the load forecast.

Typically, the load forecast is available as a probability density function (or a histogram of probability) of load level. Then, a random load pattern must be generated using load probability in order to use in time domain simulation to calculate CPS1.

Estimation of CPS1 by carrying out a time-domain simulation either using recorded data during system operation or estimated data from the probability density function is a time consuming process. Although the calculated CPS1 values are accurate, it inherits black box type characteristics where the calculation process does not provide any insight to what characteristics of load or power system has influenced the calculated CPS1 value.

1.5 Objectives of the Research

The main objectives of the research work presented in this thesis are to,

(1) analyze CPS1 to see how well it evaluates the performance of a control area, with respect to control of frequency and tie line power flows

(2) develop a novel method to estimate CPS1 given the probability distribution of load change

In order to achieve the main objectives, the following activities were carried out.

1. Investigation of literature on NERC control performance standards to learn how a control area calculates, reports and monitors its CPS1.

2. Analysis of the components of CPS1 to understand how each component relates to the performance of a power system (with respect to control of frequency and tie line power flow) and its impact on CPS1 calculation.
3. Modeling of a two-area interconnected system using the control system simulation features of PSCAD/EMTDC power system transient simulator. This test system was used to perform the necessary simulations to validate the proposed method of forecasting the CPS1 value.
4. Development of an approximate, yet simple, method using suitable assumptions to estimate CPS1 directly from the forecasted system load change probability distributions.
5. Validate the proposed method of forecasting the CPS1 value against time domain simulation method. In time domain simulation method, CPS1 is calculated by recording the deviations of area frequency and inter-area power flows in the test system introduced above.
6. Identify limitations of proposed method of forecasting the CPS1 value.

1.6 Thesis Overview

The thesis progressively discusses the approach employed to achieve the above objectives. Chapter 2 provides an overview of a typical power system and its control obligations. Here the functions of major subsystems of a power system are presented in brief, emphasizing various controls associated with them. Then the importance of real power and frequency control is discussed which is followed by an explanation of various types and

levels of controls deployed in an interconnected power system to achieve its control obligations. Finally the details of the two-area test system, which was used to perform the necessary simulations to validate the concepts developed, are presented.

Chapter 3 focuses on the first main objective of the thesis mentioned in section 1.5. It investigates the literature on NERC CPS to learn how a control area calculates, reports and monitors is CPS1. Then it follows with an analysis of the components of CPS1 to see how each component,

- assesses the performance of an interconnected system with respect to its control obligations , and
- contributes towards the final value of CPS1.

Chapter 4 lays the foundation for the second main objective mentioned in section 1.5, by proposing two alternative methods of estimating CPS1, without carrying out a time domain simulation. One of the proposed methods could be used to estimate CPS1 for a given multi-step-load-change when load change values are known with the time of occurrence of each change. However if only the load change values are known in a multi-step-load-change, then the other proposed method could be used to estimate CPS1 under certain assumptions.

Building on the later method introduced in Chapter 4, Chapter 5 proposes a method of estimating CPS1 given the probability density function of load. A case study is presented to see the accuracy of the proposed method where the CPS1 values estimated from this method is compared against time domain simulation results. The reasons for the deviations of the results and the means by which the errors could be reduced are also discussed. The validity

of the assumptions made and the limitations of the proposed method are critically analyzed by way of few sensitivity analysis presented at the end of the chapter.

Chapter 2

Frequency Control and Interconnected Power System Operation

2.1 Overview of a typical Power System

Constancy of frequency and constancy of voltage are two primary requirements of a power system, which determine the quality of power supply. In order to meet the above requirements, several levels of controls are deployed in a typical power system, which often involve complex equipment and associated complex control algorithms. Generation, transmission, sub-transmission, distribution and loads are the main constituents of a power system. Electricity is produced at generating stations and is transmitted to consumers through a complex network, made up of transmission, sub-transmission and distribution grids, which include transmission lines, transformers, switching devices and etc.

Three-phase ac generators, play the primary role in generation by converting mechanical energy to electric energy. The source of the mechanical energy may be water, steam, gas, wind, etc. A turbine converts the energy of running water, steam, gas or wind into the mechanical energy that drives the generator. Hydraulic turbines, steam turbines, gas turbines or wind mills are commonly known as prime movers.

The transmission system interconnects generating stations at various locations to the distribution system. Loads are connected to the distribution system. Transmission lines also interconnect neighboring utilities, thus enabling economical power transfers during normal operating conditions as well as mutual emergency assistance [1].

Consumers are connected to the network at transmission, sub-transmission and distribution levels and they form the loads of the power system. Large industrial loads are

directly fed from the transmission network, whereas smaller industrial loads are served from the sub-transmission network. Other small industrial loads are served from the primary distribution network while residential and commercial customers are served from the secondary distribution network. Industrial loads are composite loads, which mainly consist of induction motors. The behavior of a composite load is a function of both voltage and frequency. Lighting, heating and cooling devices form the major portion of commercial and residential loads. As these loads are primarily resistive, they are independent of frequency and consume negligibly small reactive power.

2.2 Power System Control

Figure 2-1, which is extracted from [12], depicts the various subsystems of a power system from generation level to transmission level with the various controls related to each subsystem. The objective of the control system is to generate and deliver real and reactive power demand in an interconnected system as economically and reliably as possible, while maintaining voltages and frequency and other system variables within their permissible limits. Changes in real power mainly affect the system frequency, while reactive power is less sensitive to changes in frequency. Reactive power control is closely associated with control of system bus-voltage magnitudes. Hence the power system controllers can be classified into two categories: a) real power and frequency controllers and b) reactive power and voltage controllers.

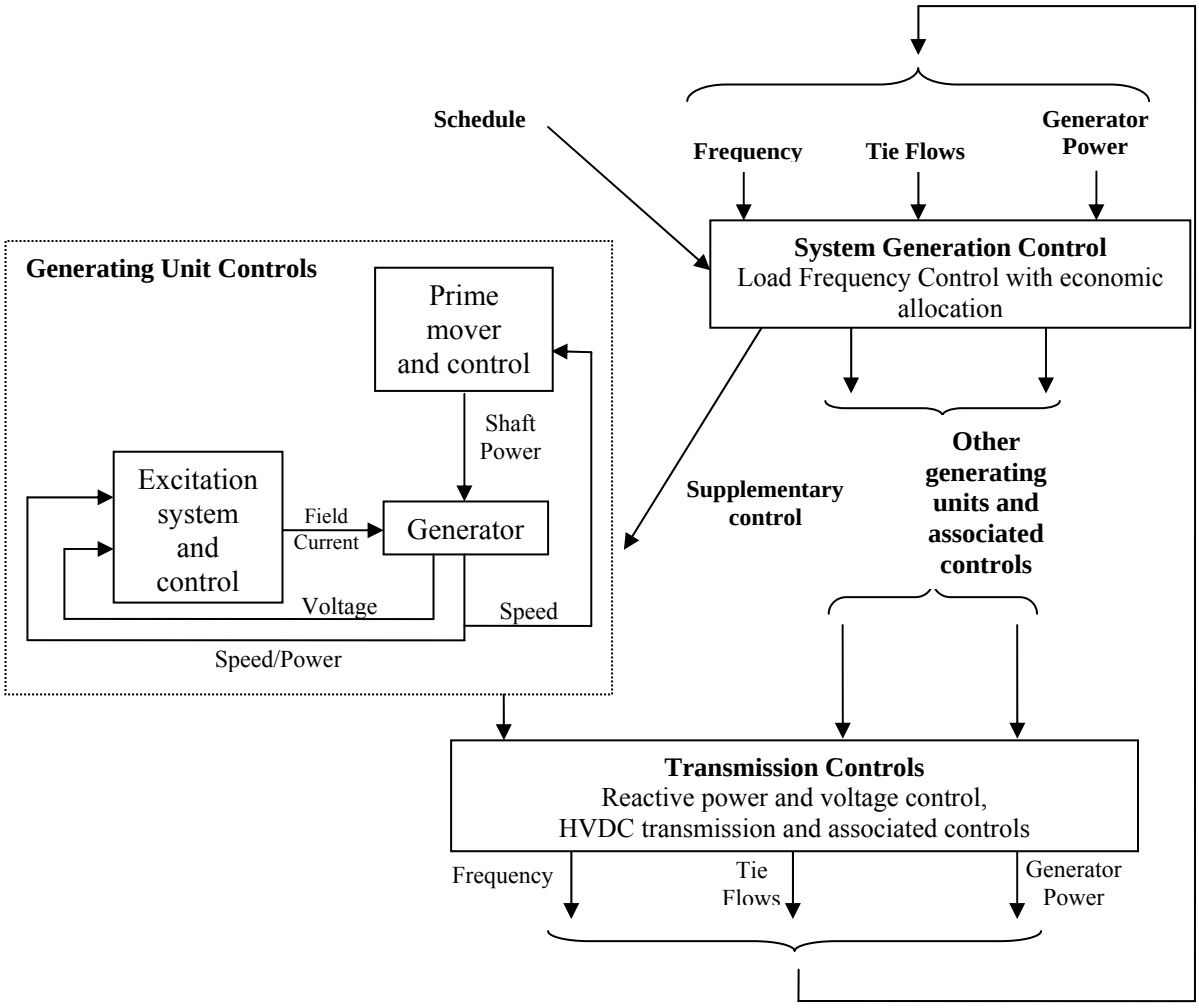

Figure 2-1: Subsystems of a power system and associated controls

Generating unit controls are employed at two stages: at each generating unit level and at generation system level. The latter enables the interconnected power system operation. Prime mover controls and excitation system controls operate directly on a generating unit. The prime mover controls are related with speed regulation, which determines the amount by which the valve/gate of turbine is opened, which in turn determines the power output of the turbine [13]. The basic function of the excitation control is to regulate generator voltage and

reactive power output. In addition to the basic function, the excitation control enhances the stability of the power system and provides protection functions by ensuring the machine is operating within its capability limits.

The primary purpose of the system-generation control is to balance the total system generation against system load and losses while maintaining the desired frequency and tie line power flows. Also an important secondary function of the system-generation control is to allocate generation according to scheduled generation dispatch [2], [15]. The transmission controls include power and voltage control devices such as static VAR devices, phase shifting transformers and HVDC transmission lines.

2.3 Real Power and Frequency Control

2.3.1 Generator response to load change

As discussed in section 2.2, real power control is closely related to frequency control. Hence, in order to maintain the system frequency at its targeted value, the real power produced should always be controlled to balance the load and generation. In order to understand the relationship between real power and frequency, consider an isolated generating unit (with no controls acting on it) supplying an isolated load as illustrated in Figure 2-2.

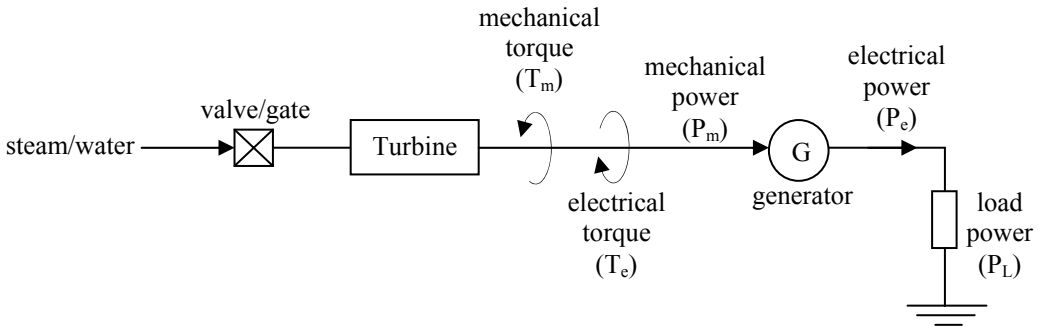

Figure 2-2: Generator supplying an isolated load (with no controls)

Now let us consider the behavior of the system depicted in Figure 2-2 in response to a load change. An increase in real power demand of the system load (P_L) will result in more electrical power being taken out of the generator. The electrical torque (T_e) will increase and if the mechanical torque of the turbines (T_m) remained unchanged, then the torque imbalance acting on the generator unit will make it to decelerate and the speed of rotation to decrease. Similarly, if more mechanical energy is being delivered to a generator than the electrical energy being removed from the electrical terminals, then the excess energy will accelerate the generator and the speed of rotation will increase. Since the generating units on the system are in synchronism, a change in generator speed will result in a change in system frequency.

The magnitude of acceleration or deceleration depends on the quantity of the power mismatch and the inertia of the turbine-generator. Inertia is a physical property of each turbine-generator that defines its ability to store rotational kinetic energy [13], [16], [17] . Inertia of a rotating system is analogous to mass of a translational system. When one or more generating units are connected to the power system, the rate at which frequency changes

depends upon the magnitude of the power imbalance and the inertia of the total rotating mass and properties of the system load.

The block diagram representation of the transfer function relating generator speed, power imbalance and the inertia of the system is illustrated in Figure 2-3 [15]. Please refer Appendix A for the derivation.

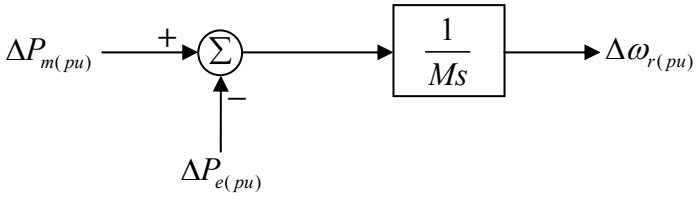

Figure 2-3: Transfer function relating speed and power

Where M = 2H; H is the Inertia Constant in W-Second/VA

s: Laplace operator

$\Delta P_{m(pu)}$: mechanical power deviation in per unit

$\Delta P_{e(pu)}$: electrical power deviation in per unit

$\Delta\omega_{r(pu)}$: rotor speed deviation in per unit

2.3.2 Load response to frequency change

The loads on a power system consist of a variety of devices, the majority of which are resistive and/or inductive [13]. Electrical power of some of these loads depends on the frequency[2], the sensitivity of which depends on the frequency-load characteristics of all the

[2] Frequency and speed are used interchangeably in this thesis to represent system frequency and generator rotor speed. Moreover, the values of these two quantities are equal in per unit terms.

devices connected to the power system. The frequency-dependent characteristic of a composite load may be approximated by the following linear relationship [18].

$$\Delta P_e = \Delta P_L + D\Delta\omega_r$$

where
ΔP_L : non-frequency-sensitive load change
$D\Delta\omega$: frequency-sensitive load change
D : load damping constant

where, D is expressed as,

$$D = \frac{\%\text{ change in load}}{1\%\text{ change in frequency}}$$

As an example, if D = 2, then a 1% change in frequency would cause a 2% change in load active power.

Now the effect of load damping could be included in Figure 2-3 to obtain the block diagram representation of the transfer function given in Figure 2-4 [15].

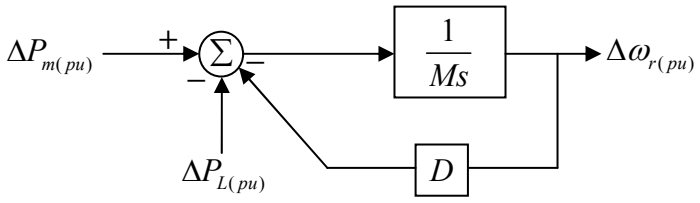

Figure 2-4: Transfer function including the effect of load damping

The two blocks in Figure 2-4 can be combined to obtain the transfer function representation shown in Figure 2-5.

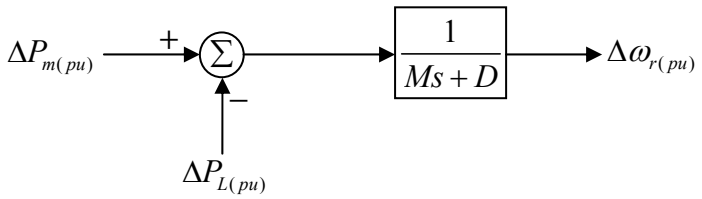

Figure 2-5: Transfer function including the effect of load damping (reduced form)

From Figure 2-5, it can be observed that with no frequency control mechanism in place, a load change will result in a steady-state frequency error whose value will be determined by the load damping constant (D). The steady- state speed deviation is such that the change in load is exactly compensated by the variation in load due to frequency sensitivity.

2.3.3 Speed Governing

The basic function of a governor is to control speed (i.e. frequency). The power output of a turbine under normal steady-state operation is set by the speed reference (speed gear) which determines the amount by which the valve/gate is opened [19], [20], [21]. When there is an imbalance between the mechanical power and the electrical power, the speed of the machine deviates from the nominal value. This speed error is sensed by the speed transducer and produces a signal proportional to the change in speed. Transducer output together with the reference setting determine the net governor signal, which acts to adjust the turbine input valve/gate to change the mechanical power output to bring the speed to a new steady-state value [22],[17]. Figure 2-6 shows these control actions in a block diagram.

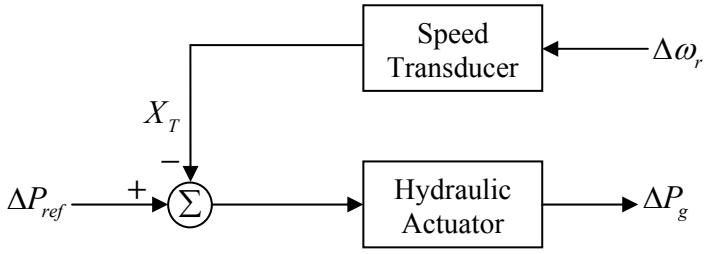

Figure 2-6: Block diagram representation of a speed governor

In Figure 2-6, $\Delta\omega_r$ is the frequency error, P_{ref} is the reference setting of generator power output, X_T is the transducer output signal and P_g is the net governor signal. Hydraulic actuator controls the valve or gate position based on the error signal (P_{ref} - X_T). The transducer together with the actuator is known as the speed governor. Figure 2-7 illustrates a generator with a turbine speed governor, supplying an isolated load.

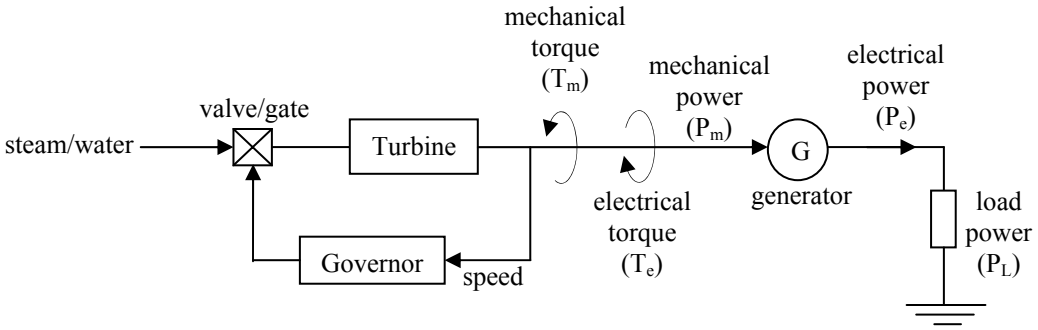

Figure 2-7: Generator with a speed governor supplying an isolated load

Governors are of two types: Isochronous governors and speed droop governors [15]. An isochronous governor is used when a single generator is supplying an isolated load whereas speed droop governors are used when two or more generators are connected in parallel.

2.3.3.1 Isochronous Governors

Figure 2-8 shows the schematic of an isochronous governor; where the frequency error is amplified (by a factor of K) and integrated over time to produce a control signal (ΔY) which actuates the valve/gate [12], [15].

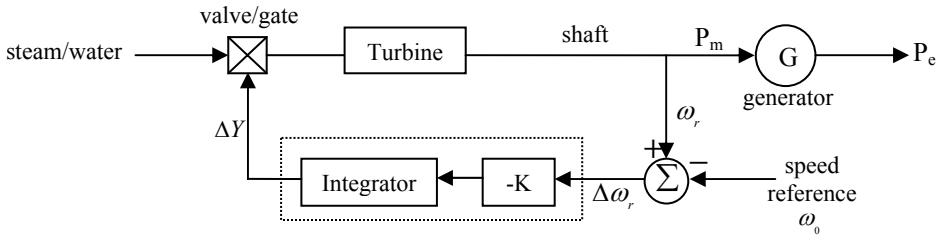

where, Y is the valve/gate position

Figure 2-8: Schematic block diagram of an isochronous governor

When there is a change in load causing a change in frequency, the isochronous governor will adjust the turbine power appropriately so that the frequency will return to its reference value. The isochronous governor is useful when the generator supplies an isolated load. However, if there are more than one generating unit connected to the same system each having an isochronous governor, they would compete with each other, each trying to control system frequency to its own setting. In practice it is not possible to set identical speed references. Therefore, this competition between governors could cause undesirable fluctuations in the generator speeds.

2.3.3.2 Speed-Droop Governors

Speed-droop-governors which inherit regulation characteristics provide a simple method of load sharing between the generating units when there are two or more units connected in parallel [15]. Figure 2-9 which is extracted from [12] is a schematic diagram of a speed-droop governor, where a steady-state feedback loop is added around the integrator to obtain the speed-droop characteristic. At a given speed, the power output of the generator could be set to any desired value by adjusting the "*load reference setpoint*" [20]. In practice this is achieved by operating a "speed-changer motor" which is also known as a "servomotor". By changing the set-point of the servomotor, the desired dispatch at nominal frequency can be scheduled.

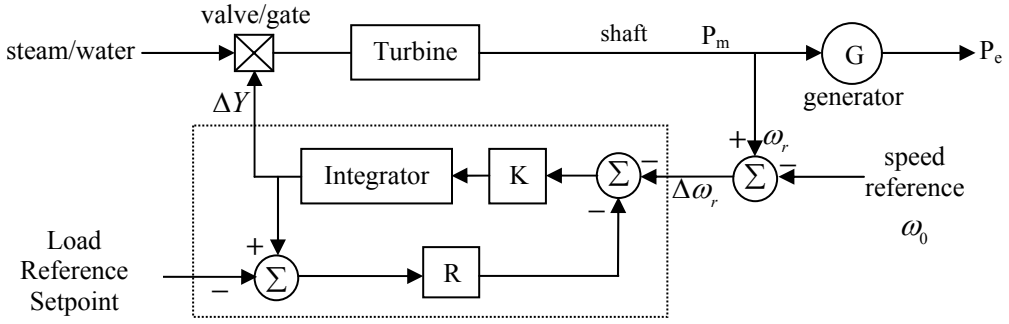

Figure 2-9: Schematic diagram of a speed-droop governor

Schematic diagram of a speed-droop governor shown in Figure 2-9 could further be reduced to obtain the schematic diagram shown in Figure 2-10.

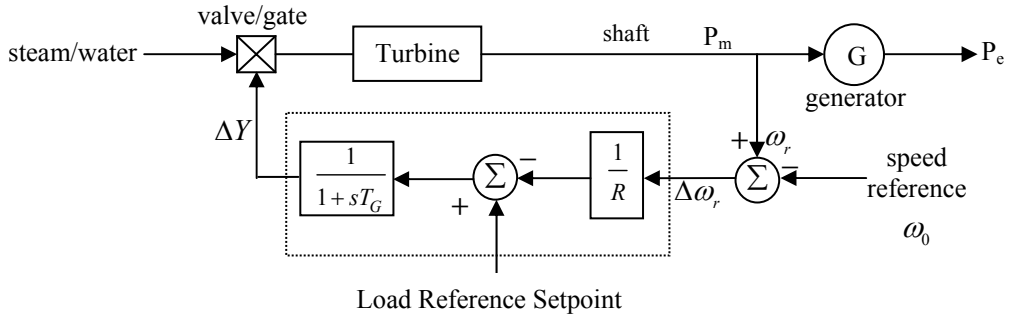

Where, $T_G = \dfrac{1}{KR}$

Figure 2-10: Schematic of a speed-droop governor with reduced governor transfer function

Constant value, R, is referred to as the speed regulation or the droop setting of the governor [22]. It is usually expressed in percentage as,

$$R = \frac{Percent\ speed\ or\ frequency\ change\ (\Delta\omega)}{Percent\ power\ output\ change\ (\Delta P)}$$

For example, if a 100MW generator has a droop setting of 5%, then for a 5% change in frequency, the turbine power output will change by 100MW.

When there are two or more generating units supplying system load, the change in generation output for a change in steady state frequency will be determined by the droop characteristics of each governor connected to generating units. Therefore, droop characteristics provide a simple way to share the generator output among the generating units [14]. However, this will result in a steady state frequency error as explained in section 2.3.4.

2.3.4 Combined speed regulating characteristic

Transfer function block diagram of the system equivalent for load frequency control shown in Figure 2-11 could be easily derived from the transfer function block diagram shown in Figure 2-5 [15].

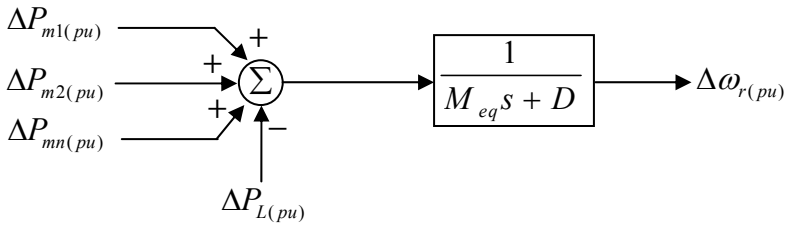

Figure 2-11: Transfer function of system equivalent

Where,

M_{eq}: sum of the inertia constants of all the generating units

D: damping constant of the total system load

For the above system, it could be shown that at steady state,

$$(\Delta P_{m1} + \Delta P_{m2} + ... + \Delta P_{mn}) - \Delta P_L = D\Delta\omega_{ss} \quad (2.1)$$

Where $\Delta\omega_{ss}$ is the steady-state frequency deviation

According to the relationship between governor droop, generator speed and generator power output described in section 2.3.3.2,

$$\Delta P_m = \frac{\Delta\omega_{ss}}{R} \quad (2.2)$$

Using(2.2), (2.1) can be re-written as,

$$\Delta\omega_{ss}\left(\frac{1}{R_1}+\frac{1}{R_2}+.....+\frac{1}{R_n}\right)-\Delta P_L = D\Delta\omega_{ss} \tag{2.3}$$

Where R_1, R_2,…….. ,and R_n are the droops of governors connected to the generators 1, 2,…..,and *n* respectively.

From (2.3), the steady-state frequency deviation following a load change of ΔP_L could be found as,

$$\Delta\omega_{ss} = \frac{-\Delta P_L}{\left(\frac{1}{R_{eq}}+D\right)} \tag{2.4}$$

Where, $\frac{1}{R_{eq}} = \frac{1}{R_1}+\frac{1}{R_2}+.....+\frac{1}{R_n}$

According to (2.4), the combined speed regulating characteristic of a power system depends on the combined effect of droops of all the generator speed governors and the damping properties of all the loads in the system.

2.3.5 Levels of frequency control

In general, three levels of controls are used to maintain the balance between load and generation, namely, primary frequency control, secondary frequency control and tertiary frequency control [23]. Tertiary frequency control refers to adjusting load reference set point manually; whereas, primary control is associated with governor droop control and secondary control is associated with the automatic generation control as explained in sections 2.3.5.1 and 2.3.5.2, respectively [23].

2.3.5.1 Primary Frequency Control

When two or more generators with speed-droop governors are operating in parallel, all of them will respond to a sudden change in load, irrespective of the location of the load change. The contribution of each generator to the load change will be determined by the speed-droop characteristic of each generating unit. Therefore, with speed-droop governor action, a change in system load will result in a steady-state frequency deviation as illustrated earlier in section 2.3.4.

This speed control function provided by speed-droop governors are referred to as "Primary Speed/Frequency Control". This control function is a local automatic control deployed on almost all the generating units in the system. This control function is particularly important to stabilize the frequency following large generation or load outages. Hence, primary frequency control function is considered to be crucial for the stability of the power system [23].

2.3.5.2 Secondary Frequency Control

As explained in section 2.3.5.1, primary speed control function controls and avoids the occurrence of any undesirable frequency excursions, following a system load change. Re-establishing the system frequency to its targeted value must be done by adjusting the load reference set-point of a generator. This control function is referred to as the "Secondary Speed/Frequency Control". Since the output of the generator needs to be changed automatically to match the continually changing load demand, this control function is also

known as “Automatic Generation Control” [24]. In a control area, automatic generation control is usually implemented on selected generating units.

2.3.6 Automatic Generation Control

2.3.6.1 Automatic Generation Control in a single-area system

In a single-area system, the primary objective of Automatic Generation Control (AGC) is to bring the system frequency back to its nominal value. This is achieved by adding an integral control, which acts on the load reference set points of the governors selected to be on AGC. Figure 2-12, which is extracted from [12], shows an isolated power system, with two governor units, where AGC is implemented on one of them. The integral control action ensures zero frequency error in the steady state.

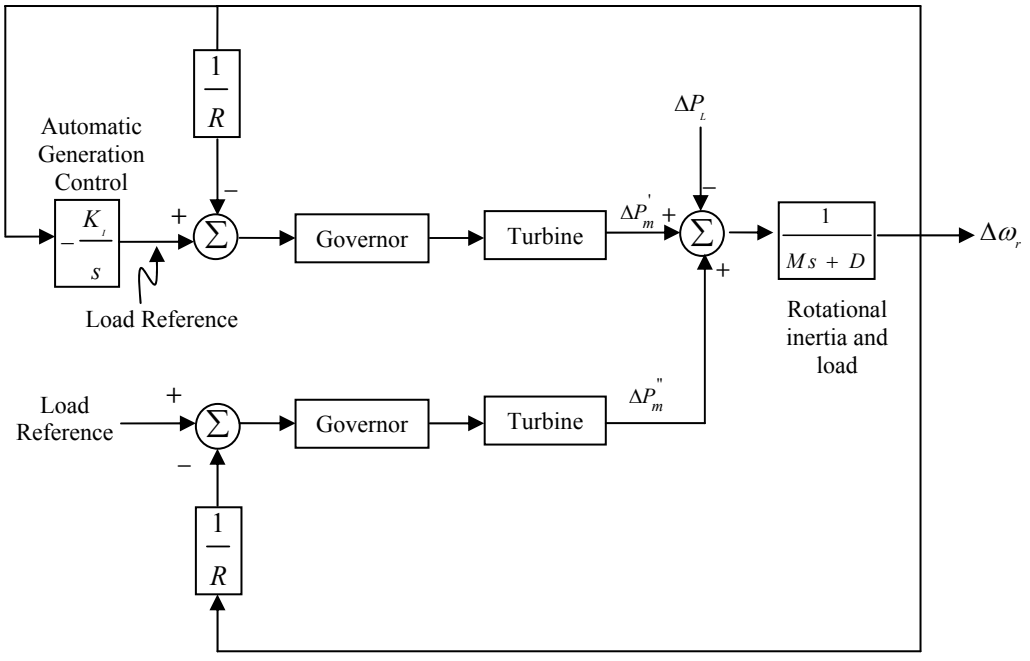

Figure 2-12: Implementation of AGC in an isolated power system

2.3.6.2 AGC in a two-area system

In order to form the fundamentals of AGC implementation, first the performance of a two-area system with only primary frequency control is considered.

Figure 2-13 illustrates a simple 2-area system. Area A and area B are the two control areas, which are connected by a lossless tie line with a reactance X_t. It is assumed that the generators in each area are closely coupled internally and swing in union. Also, the generator turbines are assumed to have the same response characteristics. Under the above assumptions, each area could be represented by an equivalent single generator, which is a voltage source (E_A, E_B), behind an equivalent reactance (X_A, X_B), as viewed from the tie line. The electrical equivalent of the system is shown in Figure 2-14.

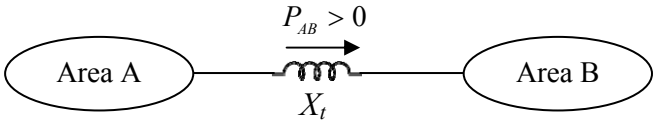

Figure 2-13: Two-area interconnected system

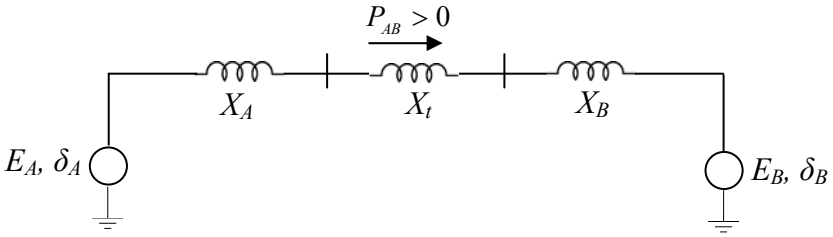

Figure 2-14: Electrical equivalent of the two-area interconnected system

The real power flow over the tie line from area A to area B during normal operation is given by,

$$P_{AB} = \frac{|E_A||E_B|\sin\ \delta_{AB}}{X_{AB}} \tag{2.5}$$

Where $X_{AB} = X_A + X_t + X_B$, $\delta_{AB} = \delta_A - \delta_B$, $\delta_A = \delta_A^0 + \Delta\delta_A$, $\delta_B = \delta_B^0 + \Delta\delta_B$

Equation (2.5) can be linearized for a small deviation in the tie-line flow ΔP_{AB} from the nominal value, i.e.,

$$\Delta P_{AB} = \left.\frac{dP_{AB}}{d\delta_{AB}}\right|_{\delta_{AB}^0} \times \Delta\delta_{AB} \tag{2.6}$$

where $\delta_{AB}^0 = \delta_A^0 - \delta_B^0$

$$\Delta P_{AB} = \frac{|E_A||E_B|}{X_{AB}}\cos(\delta_A^0 - \delta_B^0)\left(\Delta\delta_A - \Delta\delta_B\right) \tag{2.7}$$

Equation (2.7) can be re-written as,

$$\Delta P_{AB} = T_{AB}\left(\Delta\delta_A - \Delta\delta_B\right) \tag{2.8}$$

where

$$T_{AB} = \frac{|E_A||E_B|}{X_{AB}}\cos(\delta_A^0 - \delta_B^0) \tag{2.9}$$

is the *synchronizing torque coefficient* or the *electrical stiffness* of the tie-line.

Figure 2-15, which is extracted from [12] gives the block diagram representation of the two-area interconnected system, with only primary speed control action in each area. It is assumed that the equivalent generator in each area has an inertia constant M_{eq}, which is equal

to the sum of the inertia constants of all the generating units. It is also assumed that the generator in each area is driven by the combined mechanical outputs of the individual turbines. M_A and M_B represent the inertia constants of the equivalent generators in area A & area B respectively. Similarly, the effects of the system loads are lumped to a single damping constant D. D_A and D_B represent the damping constants of area A and area B respectively. The effective speed droop of the governors in area A and B are R_A and R_B respectively.

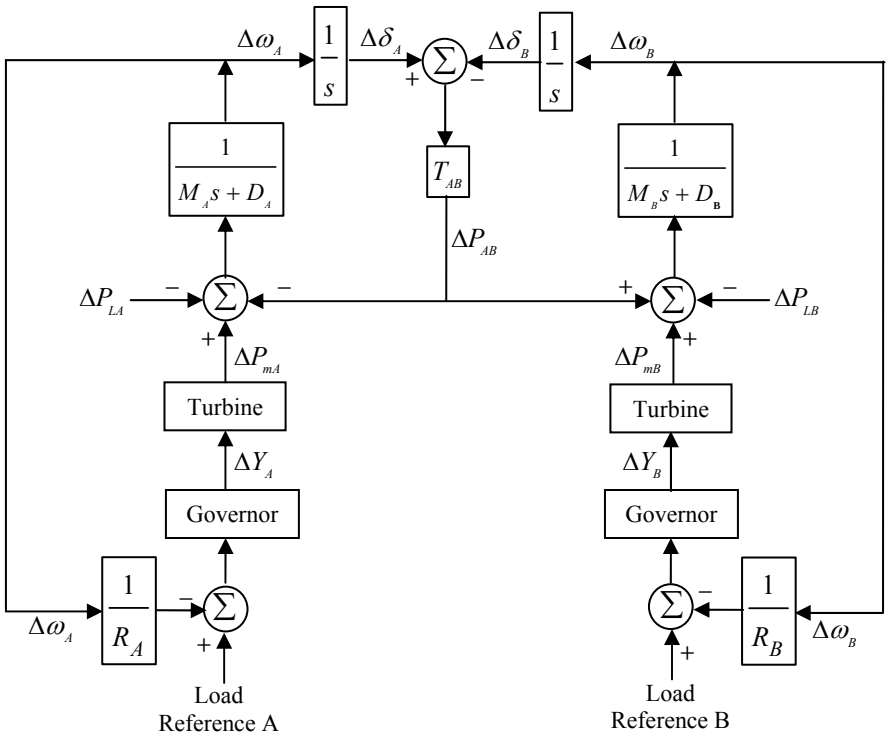

Figure 2-15: Two-area system with only primary speed control

At the steady-state, both areas will have the same steady-state frequency deviation.
For a load change of ΔP_{LA} in area A,

$$\Delta\omega = \Delta\omega_A = \Delta\omega_B \tag{2.10}$$

For area A

$$\Delta P_{mA} - \Delta P_{LA} - \Delta P_{AB} = D_A \times \Delta \omega_A \tag{2.11}$$

And for area B

$$\Delta P_{mB} + \Delta P_{AB} = D_B \times \Delta \omega_B \tag{2.12}$$

The change in mechanical power is determined by the governor speed-droop characteristics given by,

$$\Delta P_{mA} = -\frac{\Delta \omega_A}{R_A} \tag{2.13}$$

$$\Delta P_{mB} = -\frac{\Delta \omega_B}{R_B} \tag{2.14}$$

Substituting equation (2.13) and (2.14) in equation (2.11) and (2.12) respectively will result in,

$$\Delta \omega = \frac{-\Delta P_{LA}}{(1/R_A + D_A) + (1/R_B + D_B)} = \frac{-\Delta P_{LA}}{\beta_A + \beta_B} \tag{2.15}$$

and

$$\Delta P_{AB} = \frac{-\Delta P_{LA}(1/R_B + D_B)}{(1/R_A + D_A) + (1/R_B + D_B)} = \frac{-\Delta P_{LA}\beta_B}{\beta_A + \beta_B} \tag{2.16}$$

where $\beta_A = \frac{1}{R_A} + D_A$ and $\beta_B = \frac{1}{R_B} + D_B$

β_A and β_B are called the composite frequency characteristics of area A and area B respectively.

According to (2.15) and (2.16), with only primary speed control, a change of power in an area will be met by the change in generation in both areas, resulting in a change in the tie-line power flow and a change in the system frequency.

The basic objective of secondary speed control is to adjust the active power production of the generating units to restore the frequency and the power interchanges with neighboring areas to their targeted values, following an imbalance. Ideally, only the generating units that are located in the area where the imbalance originated should participate in this control as it is the responsibility of each area to maintain its load and generation in balance.

Primary speed control acts generally in the time frame of 2 to 30 seconds after a disturbance [14]. Secondary speed control action takes effect in the time frame of 15 seconds to 15 minutes and adjusts the load reference settings of units on AGC [14] . Therefore the output power of generators on AGC is adjusted which results in overriding the system frequency set by the primary speed control action. Also in the mean time, the generation of all other units not on AGC is restored back to their scheduled values.

Two-area system is a special occasion of a multi-area system and all the concepts developed above could be generalized to systems with more than two areas.

2.3.7 Tie-Line Bias Control

In North American power systems, “Tie-Line Bias Control” is the accepted strategy used to implement AGC in each area of a multi-area interconnected system [24]. There are three main functions of tie-line bias control, which are listed below [25],

1. allows an area to absorb its own local load changes
2. determines the steady-state response of an area to a remote load change
3. allows each area to perform its own system frequency control

In order to realize the above functions, tie-line bias control sets the required generation for each area, to be equal to the sum of area load and losses, scheduled interchange, and the area's share of support for interconnection frequency [26], [27]. The area's share of support for interconnection frequency is determined by the area frequency bias characteristic adopted by the area, which is described later in this section. Tie-line bias control uses a control signal known as an "Area Control Error" to accomplish the above control strategy.

Area Control Error or ACE is a control signal made up of the algebraic sum of a control area's power mismatch (i.e. the difference between the actual power flow and the area's scheduled power flow) and the area's natural response (i.e. area's support to the interconnection) to frequency deviations [24].

The ACE for each control area of a two-area interconnected system consisting of areas A and B could be written as,

$$ACE_A = \Delta P_{AB} - (10 \times B_A \times \Delta f) \tag{2.17}$$

$$ACE_B = \Delta P_{BA} - (10 \times B_B \times \Delta f) \tag{2.18}$$

where B_A and B_A are known as the frequency bias factors of area A and B respectively and is normally expressed as a negative value with the units MW/0.1Hz. Frequency bias factor is a measure of frequency bias characteristic of the area. The units of ACE are MW and it

represents the required change in area generation. ACE is used as the actuating signal to activate changes in the reference power set points, and when steady-state is reached, ΔP_{AB} and Δf will be zero.

Each control area tries to reduce its ACE to zero. When all areas in an interconnection do this, the interconnection will achieve its scheduled system frequency and all net interchanges will be on schedule [28].

An overall satisfactory performance is achieved when B is selected to be equal to the frequency-response characteristic, ß of the area [25], [29], [30]. That is,

$$B_A = \beta_A = \frac{1}{R_A} + D_A \tag{2.19}$$

and

$$B_B = \beta_B = \frac{1}{R_B} + D_B \tag{2.20}$$

Figure 2-16, which is extracted from [12] illustrates a two-area interconnected system with secondary speed control in both areas on selected generators.

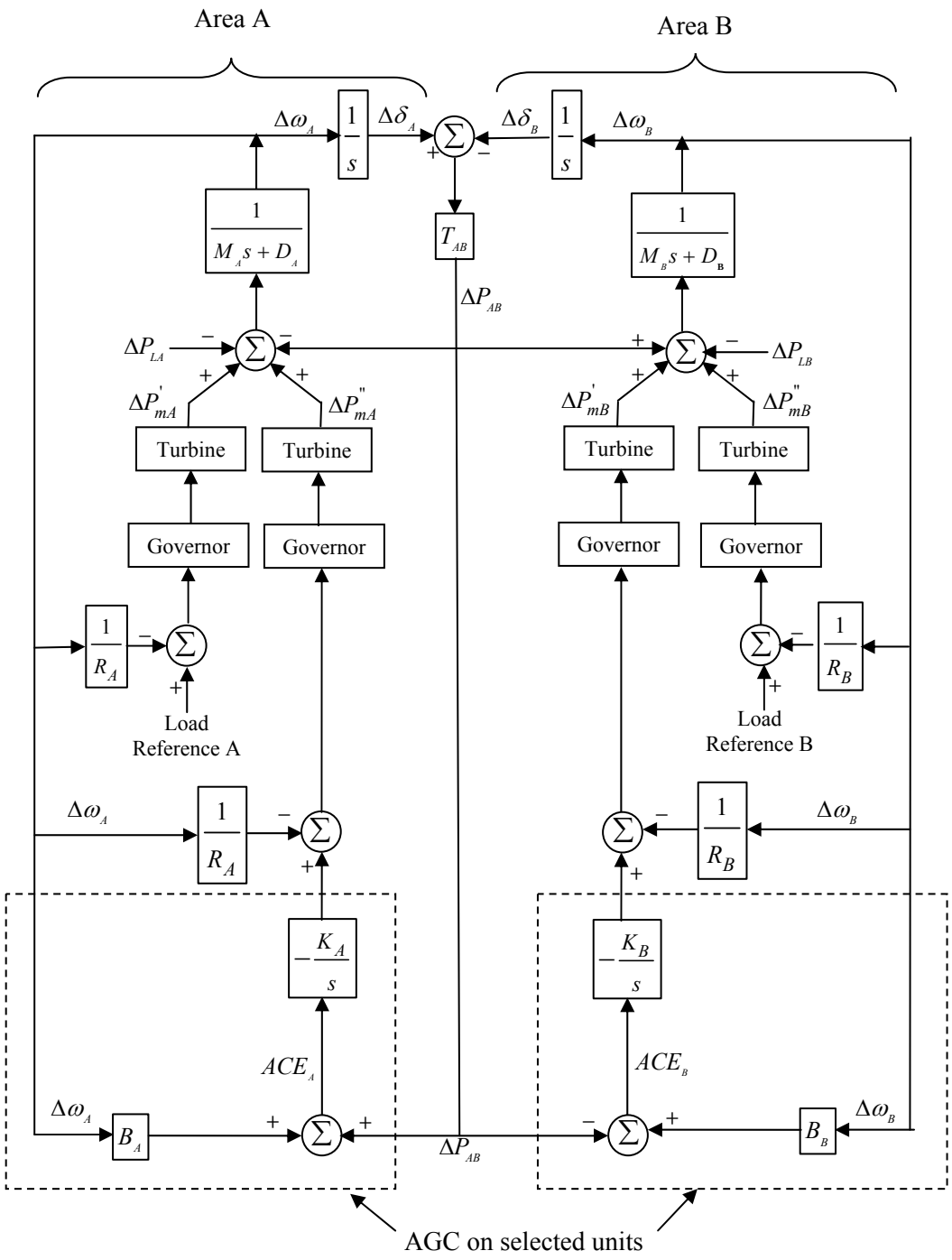

Figure 2-16: Two-area system with secondary speed control

2.3.8 Modeling a two-area interconnected power system

In order to validate the concepts developed in Chapter 4 and Chapter 5 of this thesis, the simple two-area interconnected system presented in Example 11.3 of [12] was used. The example system was similar to the two-area interconnected system shown in Figure 2-16, where primary and secondary frequency controls were deployed in both areas. The model could be simulated using any program suitable for control system simulation and in this study; the control system simulation features of PSCAD/EMTDC electromagnetic transient simulation program were used.

System parameters and the initial conditions of the system given in the example were used to construct the system in PSCAD/EMTDC, while assuming suitable and practical values for the parameters which were not specified. The absolute values were used throughout the model instead of per unit values, in order to make the modeling and analysis process simple and straightforward. Explained below are the details of the various power system components used and the assumptions made in modeling the system.

2.3.8.1 Initial Conditions

Area A and area B were the two interconnected areas. The initial loads at the nominal system frequency of 60 Hz were 20,000 MW and 40,000 MW in areas A and B respectively. Area A was operating with a spinning reserve of 1,000 MW spread uniformly over a generation of 4,000MW. Area B was operating with a spinning reserve of 1,000 MW spread uniformly over a generation of 10,000MW. The generation carrying spinning reserve in each area was on AGC control. The frequency bias factor settings were -250 MW/0.1 Hz and -500 MW/0.1 in areas A and B respectively. Area A was importing 1,000 MW from area B.

2.3.8.2 Modeling Governor-Turbine units

The generating units in each area are grouped into two categories for the purpose of modeling their governor and turbine responses. The units with only primary speed control action are modeled by a single governor-turbine model. The remaining units which are equipped with Automatic Generation Control (AGC) are modeled by another single governor-turbine model.

Generating units with reheat steam turbines and speed-droop governor are used throughout the model. Turbine parameters are assumed to be equal to the typical values for similar units given in [12]. Please refer to Appendix B for additional details of widely used turbine types in power systems.

Figure 2-17 depicts the governor-turbine arrangement used in the model. Four such units are used in the two areas, with two units in each area.

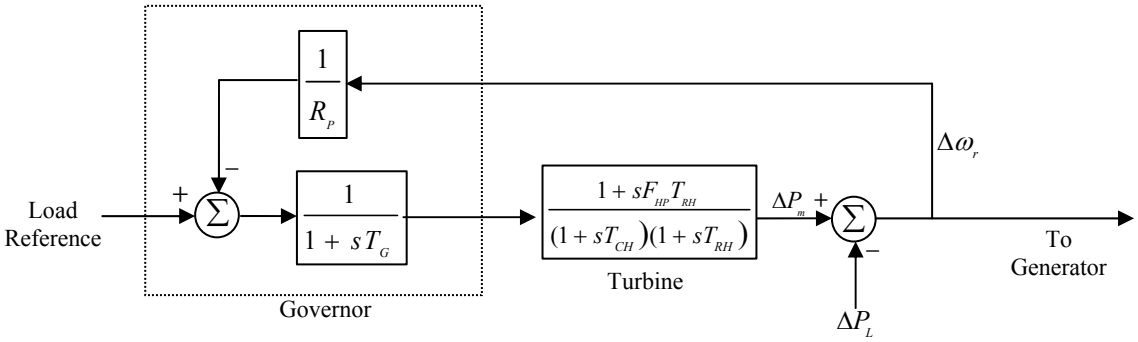

Values used for the constants:

$R_P = 0.05 \quad T_G = 0.2s \quad F_{HP} = 0.3 \quad T_{RH} = 7.0s \quad T_{CH} = 0.3s \quad F_{LP} = 0.3 \quad M = 10.0s \quad D = 1.0$

Figure 2-17: Block diagram of the governor-turbine model

2.3.8.3 Modeling Generator units

It is assumed that all generators in an area respond coherently to system changes and hence they are represented by an equivalent single generator in each area. The inertia constant of the equivalent generator in an area is assumed to be equal to the sum of the inertia constants of all the generating units and be driven by the combined mechanical outputs of the individual turbines in the area. The absolute value of *M* in each area is found using (2.21) in the simulation model. Modeling *M* in this manner enables the each area generator to respond correctly, in case of a generator tripping or addition.

$$M(MW/Hz) = \frac{total\ spinning\ generation\ capacity(MW) \times M(pu)}{nominal\ system\ frequency(Hz)} \qquad (2.21)$$

2.3.8.4 Modeling Load Damping

Similarly, the damping properties of the system load in an area is lumped to a single damping constant *D*. The load in each area is assumed to vary 1% for every 1% change in frequency. Hence, the load damping constant, $D_A = D_B = 1.0$, where D_A and D_B were the damping constants of area A and area B respectively. The change in load in MW due to load damping is calculated using (2.22) to use in the simulation model. Modeling *D* in this manner enables each area to respond correctly, in case of a load tripping or addition.

$$D(MW) = \frac{instantaneous\ load(MW) \times D(pu) \times frequency\ change(Hz)}{nominal\ system\ frequency(Hz)} \qquad (2.22)$$

2.3.8.5 Modeling Governor Droop

Similarly, the regulating characteristics of the governor units are lumped to a single droop value R. The power output is assumed to vary 100% for a 5% change in frequency. Hence, $R_A = R_B = 5.0\%$, where R_A and R_B are the droop values of area A and area B respectively. The change in generation in MW due to speed regulation is calculated using (2.22) to use in the simulation model. Modeling R in this manner enables each area to respond correctly, in case of a generator tripping or addition.

$$R(MW) = \frac{total\ spinning\ generation\ capacity(MW) \times frequency\ change(Hz)}{R(pu) \times nominal\ system\ frequency(Hz)} \tag{2.23}$$

Chapter 3
NERC Control Performance Standard 1

3.1 Control Performance Standards

The NERC Control Performance Standards (CPS) is the measure against which all control areas are evaluated. A control area is required to continuously monitor its control performance and report its compliance results at the end of each month to the NERC representative appointed to the region [31].

A control area's ACE is the basis for the calculation of CPS. ACE values used for the calculation, should reflect its actual value excluding any erroneous readings such as short excursions or "spikes" due to telemetering problems [31].

3.2 Control Performance Standard 1

Frequency Profile of an interconnection, which shows the variation of frequency with time, indicates how well generation matches load in an interconnection. Through its new CPS, NERC proposes a mathematical model for distributing control responsibility among control areas to achieve any targeted frequency profile. A targeted frequency profile can be defined in terms of frequency error averages, which is the average of the frequency deviation from the nominal system frequency, over a period of time. NERC Control Performance Standard 1 (CPS1) evaluates the performance of a control area under normal operating conditions and specifies whether the performance is satisfactory for a given frequency error.

Hence CPS1 is a frequency related parameter which imposes the following requirement on a control area [31].

> Over a given period, the average of the *clock-one-minute averages* of a control area's, "*ACE divided by ten times its bias*" times the corresponding *clock-one-minute averages* of the "*interconnection's frequency error*" shall be less than or equal to a constant [31].

This constant is given on the right-hand side of the inequality given in 3.1.

$$AVG_{period}\left[\left(\frac{ACE_i}{-10B_i}\right)_{\text{clock-one-minute-avg}} \times \left(\Delta f_i\right)_{\text{clock-one-minute-avg}}\right] \le \varepsilon_1^2 \qquad (3.1)$$

Where, i : represents the control area (e.g. i = 1, 2 for a two-area system),

AVG :average

ACE : Area Control Error,

B : Bias factor,

Δf : Clock-one-minute-average value of frequency error,

period : one year for control area evaluation or one month for Resources Subcommittee review

ε_1 : A constant derived from the targeted frequency bound

ε_1 is the targeted Root Mean Square (RMS) value of clock-one-minute-average frequency error from a schedule based on frequency performance over a given year. The bound is the same for every control area within an interconnection.

For the calculation of one-minute average values, ACE and frequency error samples are recorded at the end of each AGC cycle. The usual duration of an AGC cycle is four

seconds [12], hence clock-one-minute average can be calculated by averaging the 15 samples taken per minute.

The inequality given in (3.1) allows deciding whether a control area is in compliance with the CPS1 requirement, however, it does not provide the degree of compliance or non-compliance. In order to calculate the degree of compliance or non-compliance, CPS1[3] provides the compliance percentage as

$$CPS1 = (2 - CF) \times 100\% \tag{3.2}$$

where the frequency-related Compliance Factor, CF, is a ratio of all clock-one-minute compliance factors accumulated and averaged over a 12-month-period and then divided by the square of the target frequency bound. *i.e.*

$$CF = \frac{CF_{12-month-avg}}{\varepsilon_1^2} \tag{3.3}$$

Calculation of $CF_{12\text{-}month\text{-}avg}$ is described in Section 3.2.1.

If CPS1 is more than or equal to 100%, then NERC estimates that the control area has satisfied the compliance and area fails compliance if CPS1 is less than 100%.

3.2.1 Calculation of $CF_{12\text{-}month\text{-}avg}$

Clock-one-minute-average values of ACE and Δf for a 12-month-period form the basis for the calculation of $CF_{12\text{-}month\text{-}avg}$. Further, hourly and monthly averages of CF, calculated using clock-one-minute-average values of CF form the intermediary steps in calculating $CF_{12\text{-}month\text{-}avg}$. These steps are explained below.

[3] Note that CPS1 is used to refer the Control Performance Standard 1 as well as the compliance percentage defined by Control Performance Standard 1.

3.2.1.1 Clock-one-minute-average

Clock-one-minute-average value is the average of a control area's any valid measured variable (*i.e. ACE* and Δf) for each sampling cycle (*i.e.* an AGC cycle) during a given clock-one-minute [31]. *i.e.*

$$\left(\frac{ACE}{-10B}\right)_{\text{clock-one-minute-avg}} = \frac{1}{-10B} \times \left(\frac{\sum_{n_{\min}} ACE}{n_{\min}}\right)$$

Similarly,

$$\left(\Delta f\right)_{\text{clock-one-minute-avg}} = \left(\frac{\sum_{n_{\min}} \Delta f}{n_{\min}}\right)$$

Where, $n_{\min}$ is the number of sampling cycles in clock-one-minute.

Hence, a control area's clock-one-minute CF becomes,

$$CF_{\text{clock-one-minute}} = \left[\left(\frac{ACE}{-10B}\right)_{\text{clock-one-minute-avg}} \times \left(\Delta f\right)_{\text{clock-one-minute-avg}}\right] \tag{3.4}$$

3.2.1.2 Hourly Average

Clock-one-minute values of CF over an hour are used to compute the respective hourly average of CF [31].

i.e.

$$CF_{\text{clock-one-hour-avg}} = \left(\frac{\sum_{n_{\text{hour}}} CF_{\text{clock-one-minute}}}{n_{\text{hour}}}\right)$$

Where, n_{hour} is the number of clock-one-minute samples in clock-one-hour

By storing the clock-one-hour-average values of CF for each of the 24 hours in a day and the number of clock-one-minute samples in each hour, the control area can calculate the clock-k^{th}-hour-average for a given hour of a day (k^{th} hour of a day, where k = 1, 2,.., 24) for the period of one month. *i.e.*

$$CF_{clock\text{-}kth\text{-}hour\text{-}avg\text{-}month} = \frac{\sum_{days-in-month} \left[(CF_{clock\text{-}kth\text{-}hour\text{-}avg}) \times (n_{kth-hour}) \right]}{\sum_{days-in-month} (n_{kth-hour})}$$

Where, $n_{kth-hour}$ is the number of clock-one-minute samples in k^{th} clock-one-hour of the day

3.2.1.3 Monthly Average

By using the clock-one-hour-average for each hour of all the days in a month and the total number of clock-one-minute samples for the corresponding clock-one-hour averages of all the days in the month, the control area can calculate one-month-average value of CF [31]. i.e.

$$CF_{one\text{-}month\text{-}avg} = \frac{\sum_{hours-in-day} \left[(CF_{clock\text{-}kth\text{-}hour\text{-}avg\text{-}month}) \times (n_{kth-hour-month}) \right]}{\sum_{hours-in-day} (n_{kth-hour-month})}$$

Where, $n_{kth-hour-month}$ is the number of clock-one-minute samples for the k^{th} clock-one-hour summed for all the days in a month.

3.2.1.4 Yearly Average

Now the 12-month-average value of CF becomes [31],

$$CF_{12-month-avg} = \frac{\sum_{12months}\left[(CF_{one-month-avg})\times(n_{month})\right]}{\sum_{12months}(n_{month})}$$

Where, n_{month} is the number of clock-one-minute samples summed for all the days in a month.

If data was not collected for all minutes in an hour or for all hours in a day or for all days in a month or for all months in a year, then the summations in the above formulas should be for the number of recorded sample of minutes, hours, days and months respectively.

Moreover, in order to ensure that the average *ACE* and Δf calculated for any one-minute interval is representative of that one-minute interval, it is necessary that at least 50% of both *ACE* and Δf samples during that one-minute interval to be present. If a sustained interruption (e.g. due to loss of telemetering or computer unavailability) in data recording results in a one-minute interval not containing at least 50% of simultaneous sample pairs of *ACE* and Δf, that one-minute interval shall be excluded [31] from the calculation of CPS1.

Described in Section 3.2.1 is the practical method of estimating CPS1. However for theoretical analysis presented in this thesis, it is assumed that

a) no erroneous data exists in any of the sampling cycles

b) each month of the 12-month-period consists of equal number of days

Under the above assumptions, (3.3) could be written in terms of clock-one-minute values of CF as,

$$CF = \frac{1}{\varepsilon_1^2}\left(\frac{\sum CF_{\text{clock-one-minute}}}{N}\right) \tag{3.5}$$

where N is the total number of clock-one-minute samples of CF values during a 12-month-period.

3.2.2 Data Reporting

Performance Standard Surveys are conducted monthly to analyze each control area's level of compliance with the CPS, which provide a relative measure of each control area's performance [31].

Each control area shall return one completed copy of CPS Form 1 which is known as "NERC Control Performance Standard Survey-All interconnections" to NERC's Resources Subcommittee member representing the region, by the tenth working day of the month following the month reported [31].

Using data derived from digital processing of the ACE signal, each control area will complete the above form with the following data and information:

a) Clock-one-hour average CF for each of the 24-hour period and the total number of samples in each hourly average

b) Monthly CF

c) Rolling 12-month CF

d) Percentage CPS1 for rolling 12-month

3.3 Analysis of the components of CPS1

According to (3.2), CPS1 for a given area is a linear function of CF for the same area. The linear relationship between CPS1 and CF is illustrated in Figure 3-1.

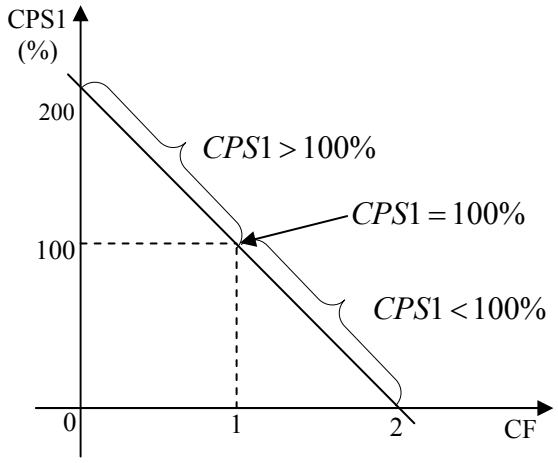

Figure 3-1: Relationship between CPS1 and CF

As depicted in Figure 3-1, when CPS1≥100, then CF≤1. Therefore, in order to be in compliance with NERC criteria, CF should be less than or equal to 1.

Now let's obtain the relationship between CF, Δf and ΔP.

As illustrated in section 2.3.7, ACE relates to Δf and ΔP as given in (3.6).

$$ACE = \Delta P - (10 \times B \times \Delta f) \tag{3.6}$$

Now substituting (3.6) in (3.4),

$$CF_{\text{clock-one-minute}} = \left[\left(\frac{\Delta P - (10 \times B \times \Delta f)}{-10B} \right)_{\text{clock-one-minute-avg}} \times \left(\Delta f \right)_{\text{clock-one-minute-avg}} \right]$$

$$CF_{\text{clock-one-minute}} = -\frac{1}{10B}\left[\left(\Delta P\right)_{\text{clock-one-minute-avg}} \times \left(\Delta f\right)_{\text{clock-one-minute-avg}}\right] + \left[\left(\Delta f_{\text{clock-one-minute-avg}}\right)\right]^2 \tag{3.7}$$

Substituting (3.7) in (3.5),

$$CF = -\frac{1}{10B\varepsilon_1^2 N^2}\left[\sum\left\{\left(\Delta P\right)_{\text{clock-one-minute-avg}} \times \left(\Delta f\right)_{\text{clock-one-minute-avg}}\right\}\right] + \frac{1}{\varepsilon_1^2 N^2}\left[\sum\left(\Delta f\right)_{\text{clock-one-minute-avg}}\right]^2 \tag{3.8}$$

For simplicity, (3.8) can be written as,

$$CF = k_1 \Sigma\left(\Delta P_{1M} \times \Delta f_{1M}\right) + k_2 \Sigma\left(\Delta f_{1M}\right)^2 \tag{3.9}$$

Where ΔP_{1M} and Δf_{1M} stand for clock-one-minute average value of ΔP and clock-one-minute average value of Δf respectively. Also $k_1 = -\frac{1}{10B\varepsilon_1^2 N^2}$ and $k_2 = \frac{1}{\varepsilon_1^2 N^2}$ are both positive constants.

Now, (3.9) could be analyzed to understand how the average behavior of a power system relates to CF, by considering different ranges of values for $\Sigma\,(\Delta P_{1M} \times \Delta f_{1M})$ and $\Sigma\,(\Delta f_{1M})^2$.

In a control area, if $\Sigma\,(\Delta P_{1M} \times \Delta f_{1M})$ is positive, it is an indication that the area is receiving help. On the other hand, if $\Sigma\,(\Delta P_{1M} \times \Delta f_{1M})$ is negative, it indicates that the area is giving help. This is illustrated in Figure 3-2 below.

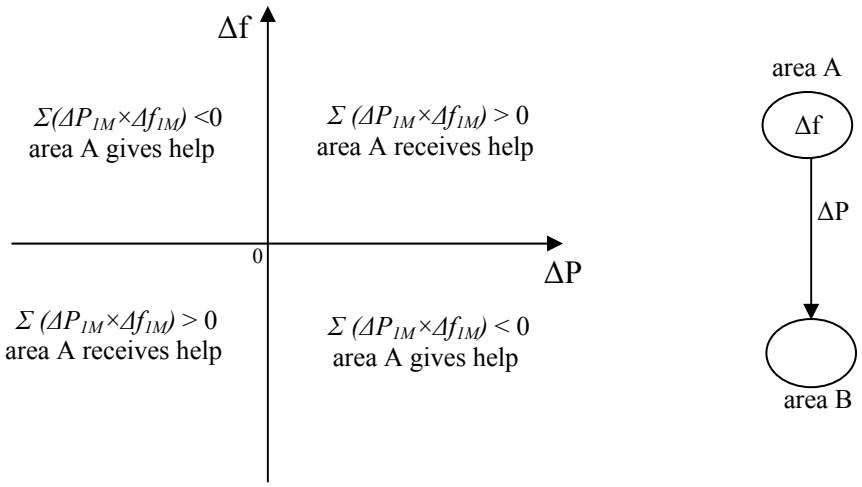

Figure 3-2: $\Sigma(\Delta P_{1M} \times \Delta f_{1M})$ in different quadrants

Hence, the sign of the first term, i.e. $k_1 \Sigma(\Delta P_{1M} \times \Delta f_{1M})$ in (3.9) determines whether an area receives assistance from or provides assistance to the interconnected system. The value of the second term, i.e. $k_2 \Sigma(\Delta f_{1M})^2$, is unity when Δf_{1M} is equal to the target bound. A value less than 1.0 means frequency control is tighter than the target bound and a value greater than 1 means the opposite.

Different combinations arising from all possible values of the first and second terms of (3.9) are tabulated in Table 3-1. The same table also gives the range of values of CF and CPS1 for those different combinations.

Table 3-1: Range of CF and CPS1

$K_2 \Sigma(\Delta f_{1M})^2$	$k_1 \Sigma (\Delta P_{1M} \times \Delta f_{1M})$	CF	CPS1 (%)
< 1	> 0	$0 < CF < \infty$	$-\infty < CPS1 < 200$
	= 0	$0 < CF < 1$	$100 < CPS1 < 200$
	< 0	$-\infty < CF < 1$	$100 < CPS1 < \infty$
= 1	> 0	$1 < CF < \infty$	$-\infty < CPS1 < 100$
	= 0	= 1	= 100
	< 0	$-\infty < CF < 1$	$100 < CPS1 < \infty$
> 1	> 0	$1 < CF < \infty$	$-\infty < CPS1 < 100$
	= 0	$1 < CF < \infty$	$-\infty < CPS1 < 100$
	< 0	$-\infty < CF < \infty$	$-\infty < CPS1 < \infty$

Although, in principle CPS1 value could vary between $-\infty$ and ∞, practical power systems typically have CPS1 values varying between 0 and 200. Thus, $-\infty$ and ∞ values in Table 3-1 can be replaced with 0 and 200 respectively.

The nine possibilities tabulated in Table 3-1 can be reduced to five possibilities by combining them according to the 4 possible ranges of CPS1 as shown in Table 3-2. In Table 3-2, "*Frequency Error*" and "*Nature of support to the adjacent area*" refer to the behavior of $\Sigma(\Delta f_{1M})^2$ and $\Sigma(\Delta P_{1M} \times \Delta f_{1M})$ respectively.

Table 3-2: Value of CPS1 for different conditions

Condition	Frequency Error	Nature of support to the adjacent area	CPS1 (%)
1	Equal to bound	Neutral	=100
2	Equal to bound	Receives support	<100
	Out of bound	Neutral	
	Out of bound	Receives support	
3	Within bound	Neutral	>100
	Within bound	Gives support	
	Equal to bound	Gives support	
4	Within bound	Receives support	<100 or >100
	Out of bound	Gives support	

Arguments which can be drawn from Table 3-2 are given below. In this text, obligation refers to either control of frequency or control of tie line power flows.

- If a control area meets both its obligations marginally

  then, its CPS1 is equal to 100% (Condition 1 in Table 3-2)

- If a control area meets only one of its obligations and it is met marginally, or does not meet any of its obligations

  then, its CPS1 is always less than 100%. The area does not comply with NERC criteria (Condition 2 in Table 3-2)

- If a control area meets both its obligations with a margin, or meets both its obligations and one is met marginally

  then, its CPS1 is always greater than 100%. The area complies with NERC criteria (Condition 3 in Table 3-2)

- If a control area meets only one of its obligations, and is met with a margin,

  then, its CPS1 can be less than 100% or greater than 100%. The area may or may not comply with NERC criteria (Condition 4 in Table 3-2).

Based on the above arguments, it can be concluded that a control area is assured to be in compliance with NERC criteria, as long as it meets both its obligations. On the other hand, the control is assured to be in non-compliance with NERC Criteria, if it does not meet both its obligations. However, if a control area meets only one of its obligations, then its compliance or non-compliance has to be decided based on the actual values of the terms 1 and 2 in (3.9).

Chapter 4
Estimation of CPS1

The most straightforward and accurate method of estimating CPS1 is to perform a time domain simulation using the load curve. Load curve gives the variation of load against time. Typically, load curve is available for past system operation and probability distribution of load curve is available for future operation. If time domain simulations are to be used to estimate CPS1 for future operation, then a random load curve must be generated.

As shown later in this thesis, the value of CPS1 depends on the change of load and its dependence on the value of the load is negligible. The objective of this thesis is to propose a novel method to estimate CPS1 directly from the probability distribution of the load change without performing a time domain simulation. This chapter lays the foundation for this objective, by establishing an approximate relationship between clock-one-minute values of CF and the magnitude (i.e. size) of a step load change. This relationship, which was found to be independent of time under certain assumptions, could then be used to estimate CPS1, thus making the time information redundant. Each step in this procedure is explained using simulation results obtained using the simple two-area system presented in section 2.3.8. The same test system is used to test the accuracy of the proposed procedure by comparing the results against the time domain simulation results.

4.1 Relationship between CF, its components and the magnitude of a single-step-load-change

As shown in section 3.2, CPS1 has a linear relationship with clock-one-minute values of CF (CF_{1M}). In this section, the relationship between CF_{1M} and a single-step-load-change is established using the linear 2-area control system model. As shown in (3.7), CF_{1M} is a function of Δf_{1M} and ΔP_{1M}. First the relationship between Δf, ΔP and a single-step-load-change is established by observing Δf and ΔP profiles for various magnitudes of step-load-changes. This association is then used to set up the relationship between Δf_{1M}, ΔP_{1M}, CF_{1M} and a single-step-load-change.

4.1.1 Relationship between Δf_{1M}, ΔP_{1M} and the magnitude of a single-step-load-change

Since the two area system introduced in section 2.3.8 is modeled as a linear control system, there should be a linear relationship between a single-step-load-change and Δf and ΔP. Therefore, if time variation of Δf subsequent to a single-step-load-change is known, then the time variation of Δf for any other single-step-load-change can be estimated provided that the limits of the control system (e.g. min/max outputs of generators, ramp rates, dead-band of the governor etc) are not reached. In order to demonstrate this relationship, three different step load changes of 100 MW, 500 MW and 1,000 MW were applied to area A, one load change at a time. The profiles of Δf_A, Δf_B and ΔP_{AB} with respect to time were obtained for the simulation period of 300 seconds.

The instantaneous values of Δf_A, Δf_B and ΔP_{AB} are denoted by Δf_A^i, Δf_B^i and ΔP_{AB}^i respectively. The following relationship is observed to be true at any given instant of time, throughout the simulation period.

$$\frac{(\Delta f_A^{\,i})_{500MW\_change}}{(\Delta f_A^{\,i})_{100MW\_change}} = 5 \qquad and \qquad \frac{(\Delta f_A^{\,i})_{1000MW\_change}}{(\Delta f_A^{\,i})_{100MW\_change}} = 10$$

$$\frac{(\Delta f_B^{\,i})_{500MW\_change}}{(\Delta f_B^{\,i})_{100MW\_change}} = 5 \qquad and \qquad \frac{(\Delta f_B^{\,i})_{1000MW\_change}}{(\Delta f_B^{\,i})_{100MW\_change}} = 10$$

$$\frac{(\Delta P_{AB}^{\,i})_{500MW\_change}}{(\Delta P_{AB}^{\,i})_{100MW\_change}} = 5 \qquad and \qquad \frac{(\Delta P_{AB}^{\,i})_{1000MW\_change}}{(\Delta P_{AB}^{\,i})_{100MW\_change}} = 10$$

This linear relationship is further illustrated in three graphs shown in Figure 4-1 to Figure 4-3, by the plots of time variation of $\Delta f_A^{\,i}$, $\Delta f_B^{\,i}$ and $\Delta P_{AB}^{\,i}$ respectively for the step load changes.

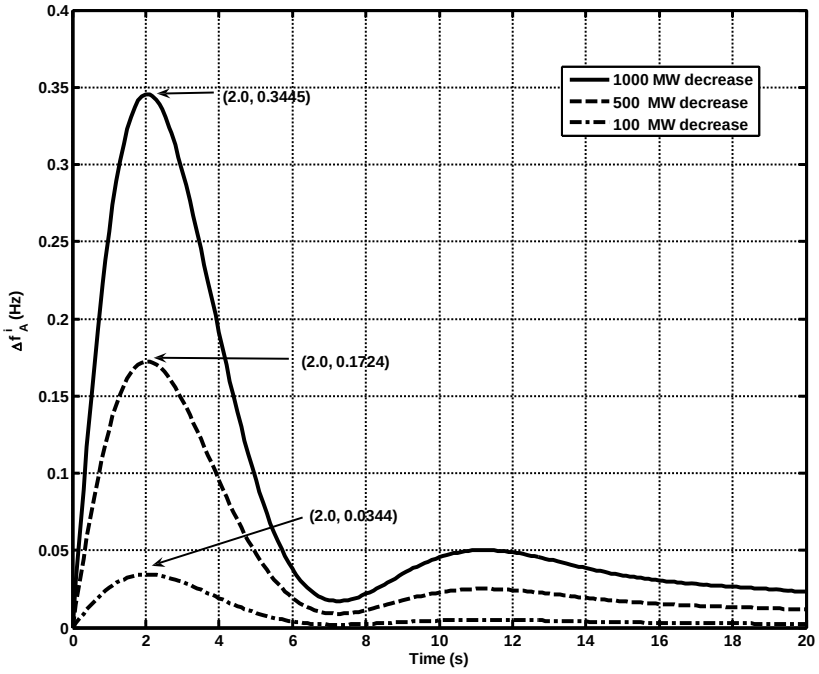

Figure 4-1: $\Delta f_A^{\,i}$ for load decrease in area A

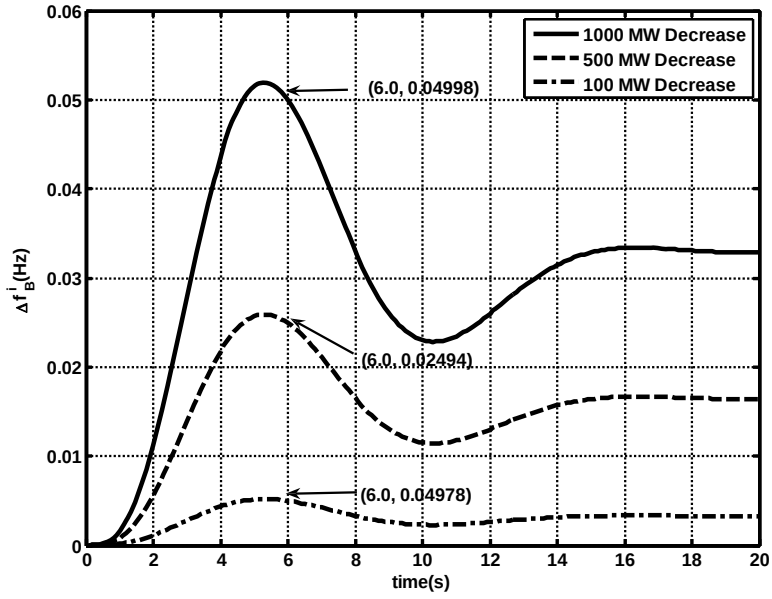

Figure 4-2: $\Delta f_B{}^i$ for load decrease in area A

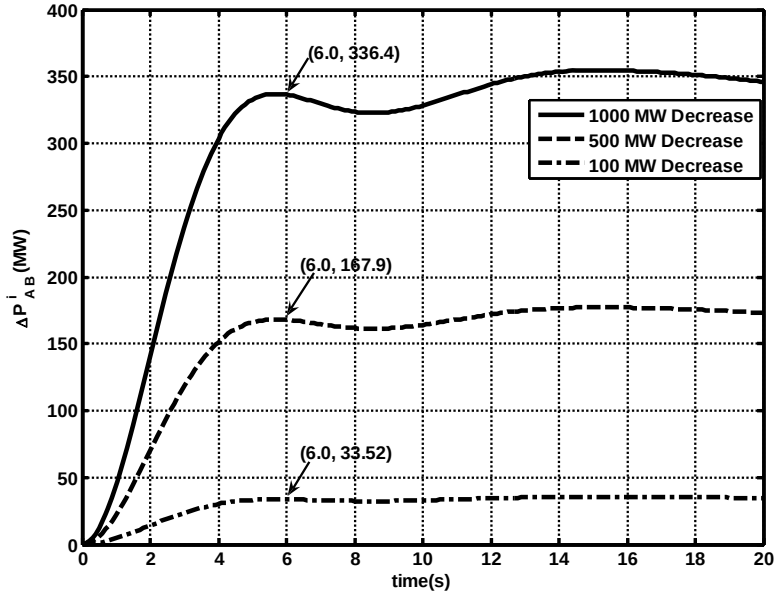

Figure 4-3: $\Delta P_{AB}{}^i$ for load decrease in area A

According to the above plots, the time variation of Δf_A^i, Δf_B^i and ΔP_{AB}^i for a 500 MW step-load-change could be obtained by scaling the respective profiles of 100 MW step-load-change by 5. Similarly the time variation of Δf_A^i, Δf_B^i and ΔP_{AB}^i for a 1000 MW step-load-change can be obtained by scaling the respective profiles of 100MW step-load-change by 10.

Based on the above observation, it can be shown that clock-one-minute-average values of Δf_A, Δf_B and ΔP_{AB} (denoted by $\Delta f_{A\text{-}1M}$, $\Delta f_{B\text{-}1M}$ and $\Delta P_{AB\text{-}1M}$ respectively) also maintain the same relationship; i.e. for 2 different step load changes in area A, $\Delta f_{A\text{-}1M}$, $\Delta f_{B\text{-}1M}$ and $\Delta P_{AB\text{-}1M}$ values are linearly proportional to the corresponding magnitudes of the step load changes. Figure 4-4 to Figure 4-6 illustrate this linearity property where $\Delta f_{A\text{-}1M}$, $\Delta f_{B\text{-}1M}$ and $\Delta P_{AB\text{-}1M}$ values for each of the first three minutes corresponding to 3 different step load changes (i.e 100MW, 500MW and 1000 MW) in area A are shown.

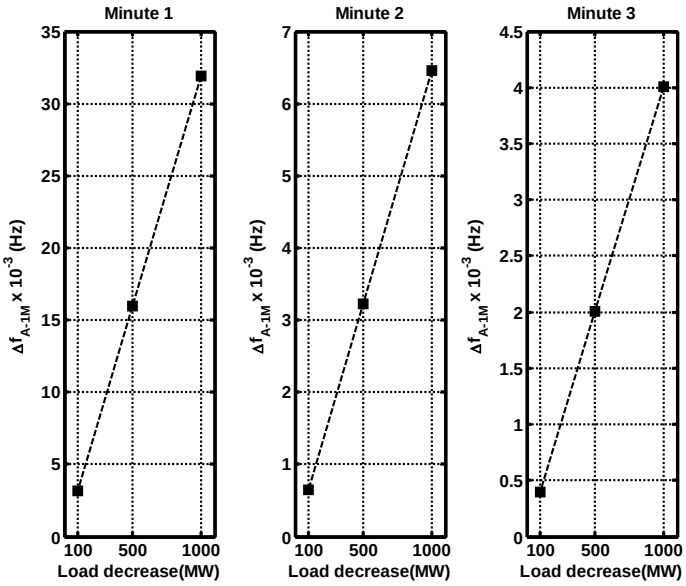

Figure 4-4: Clock-one-minute-average values of Δf_A for first three minutes

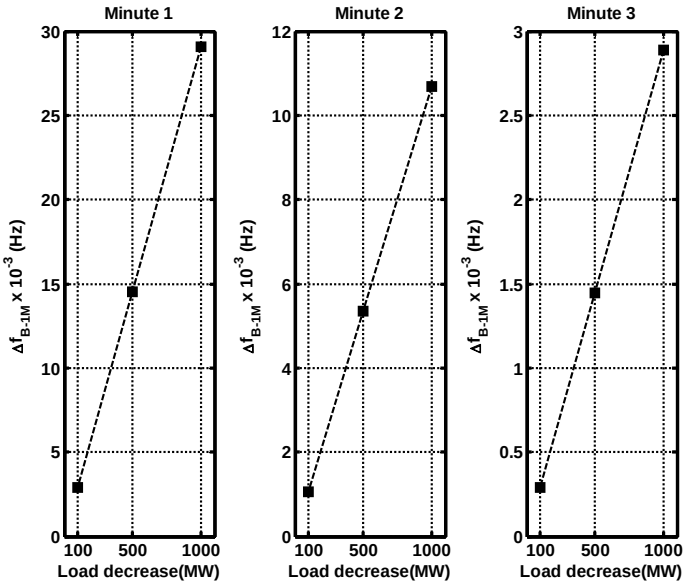

Figure 4-5: Clock-one-minute-average values of Δf_B for first three minutes

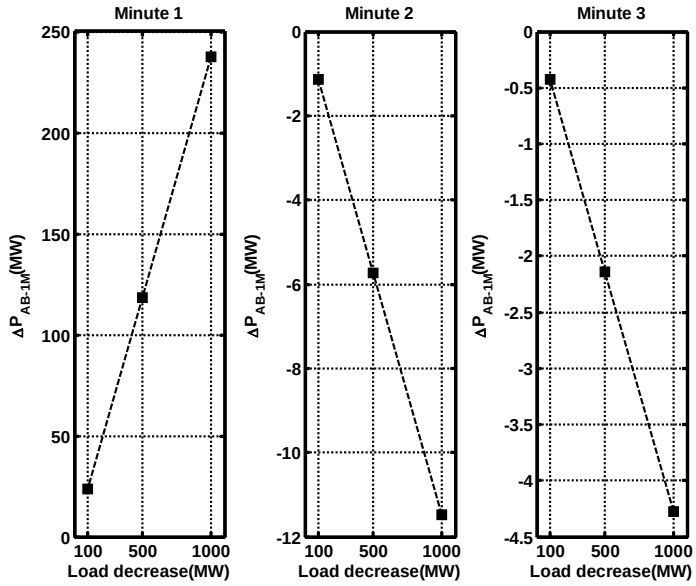

Figure 4-6: Clock-one-minute-average values of ΔP_{AB} for first three minutes

Table 4-1 to Table 4-3 summarize the normalized $\Delta f_{A\text{-}1M}$, $\Delta f_{B\text{-}1M}$ and $\Delta P_{AB\text{-}1M}$ values for the first five minutes of the step load changes. Clock-one-minute-average value of 100 MW step-load-change is taken as the base for normalization in each minute.

Table 4-1: Normalized $\Delta f_{A\text{-}1M}$

Step Load Change ΔL (MW)	Normalized $\Delta f_{A\text{-}1M}$				
	1st minute	2nd minute	3rd minute	4th minute	5th minute
±100	1.000	1.000	1.000	1.000	1.000
±500	4.999	5.001	4.998	4.997	4.995
±1000	9.995	10.008	9.990	9.987	9.979

Table 4-2: Normalized $\Delta f_{B\text{-}1M}$

Step Load Change ΔL (MW)	Normalized $\Delta f_{B\text{-}1M}$				
	1st minute	2nd minute	3rd minute	4th minute	5th minute
±100	1.000	1.000	1.000	1.000	1.000
±500	5.001	4.998	4.999	4.996	4.995
±1000	10.004	9.994	9.994	9.982	9.976

Table 4-3: Normalized $\Delta P_{AB\text{-}1M}$

Step Load Change ΔL (MW)	Normalized $\Delta P_{AB\text{-}1M}$				
	1st minute	2nd minute	3rd minute	4th minute	5th minute
±100	1.000	1.000	1.000	1.000	1.000
±500	5.001	5.012	5.001	4.976	5.012
±1000	10.003	10.055	10.002	9.890	10.056

Also, it is shown below that $\Delta f_A^{\,i}$, $\Delta f_B^{\,i}$ and $\Delta P_{AB}^{\,i}$ are equal in magnitude but opposite in sign for a step-load-increase and a step-load-decrease of the same size in a given area. See Figure 4-7 to Figure 4-9, where the plots of $\Delta f_A^{\,i}$, $\Delta f_B^{\,i}$ and $\Delta P_{AB}^{\,i}$ are shown for a 500 MW

step-load-increase and for a 500 MW step-load-decrease in area A. In order to observe the similarity, the profiles for the step-load-increase are multiplied by -1.

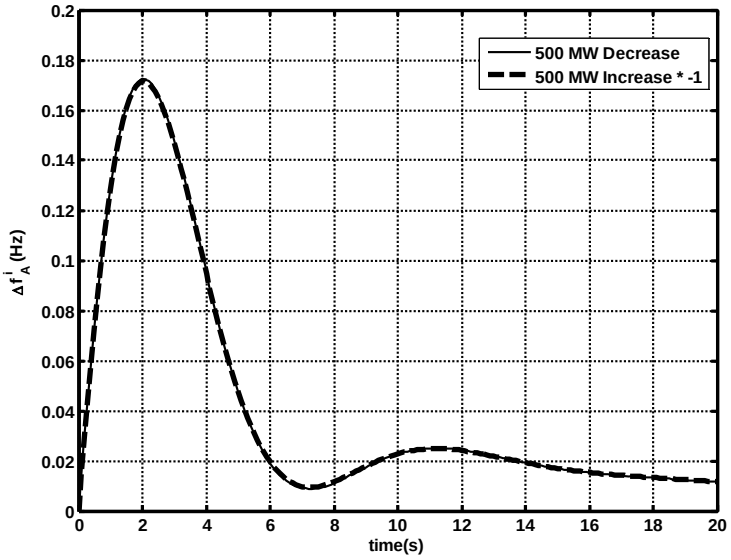

Figure 4-7: Comparison of Δf_A^i profiles

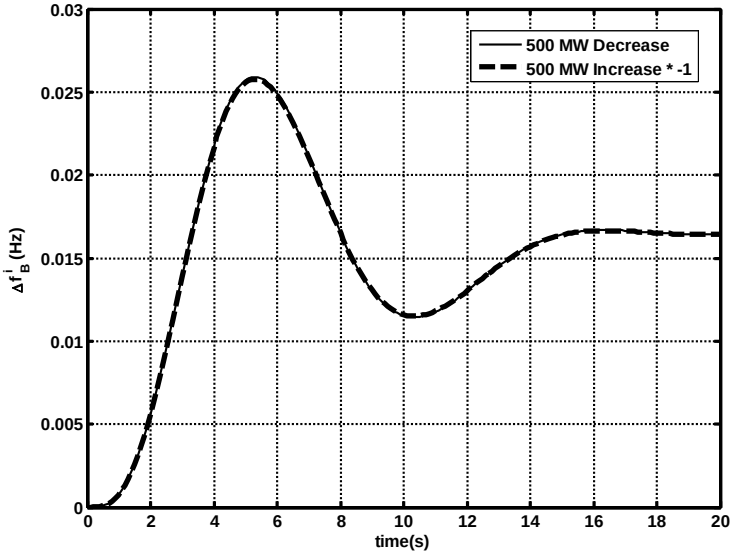

Figure 4-8: Comparison of Δf_B^i profiles

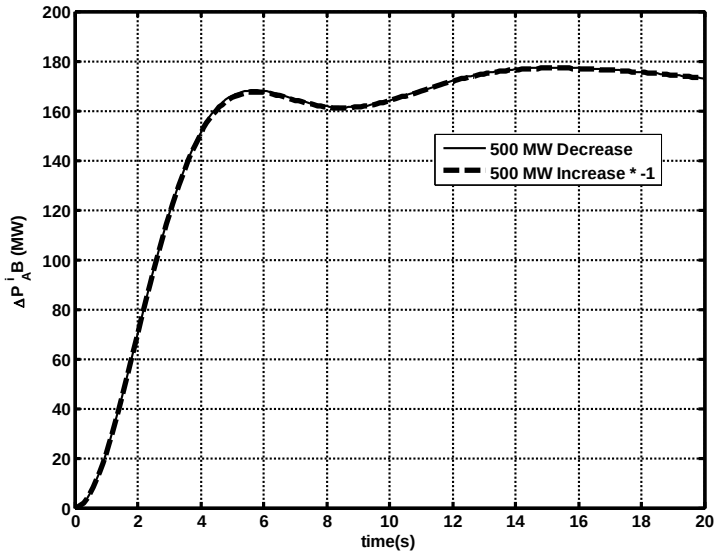

Figure 4-9: Comparison of $\Delta P_{AB}^{\ i}$ profiles

According to the above observation, it can be concluded that $\Delta f_{A\text{-}1M}$, $\Delta f_{B\text{-}1M}$ and $\Delta P_{AB\text{-}1M}$ are also equal in magnitude and opposite in sign for a step load decrease and step load increase of the same magnitude in a given area.

4.1.2 Relationship between CF_{1M} and the magnitude of a single-step-load-change

Relationship between CF_{1M} and its components in (3.7) and observations from section 4.1.1 are summarized below.

- **CF_{1M} is proportional to the term, $(\Delta P_{1M} \times \Delta f_{1M}) + (\Delta f_{1M})^2$, and**
- **Δf and ΔP are linearly proportional to the single-step-load-change.**

Based on above facts, it can be concluded that CF_{1M} following a single-step-load-change is a *quadratic* function of the magnitude of the step load change.

Figure 4-10 and Figure 4-11 plot CF_{1M} values of area A and area B (denoted by $CF_{A\text{-}1M}$ and $CF_{B\text{-}1M}$) for the first three minutes following a single-step-load-change (100 MW, 500 MW and 1000 MW) in area A. These data points are shown as solid circles.

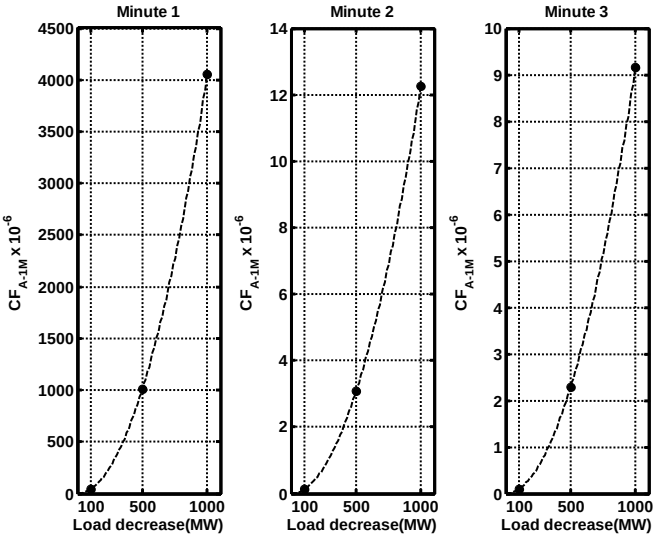

Figure 4-10: $CF_{A\text{-}1M}$ for first three minutes

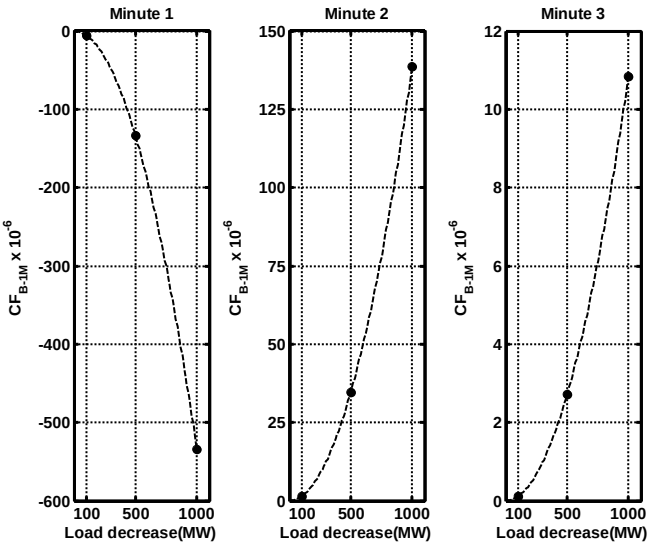

Figure 4-11: $CF_{B\text{-}1M}$ for first three minutes

CF_{1M} data points could be connected with a second order polynomial function of the type $CF_{1M} = \lambda (\Delta P_L)^2$, where, λ is a constant and ΔP_L is the magnitude of the step-load-change. This quadratic function is shown in dotted line. This shows the quadratic relationship between CF_{1M} and magnitude of the single-step-load-change.

Table 4-4 and Table 4-5 below summarize the normalized CF_{1M} values of area A and area B for a single-step-load-change in area A. CF_{1M} values corresponding to 100 MW step-load-change is taken as the base for normalization in each minute.

Table 4-4: Normalized $CF_{A\text{-}1M}$

Step Load Change ΔP_L (MW) in Area A	Normalized $CF_{A\text{-}1M}$					5-minute-average
	1st minute	2nd minute	3rd minute	4th minute	5th minute	
±100	1.000	1.000	1.000	1.000	1.000	1.000
±500	24.996	24.953	24.967	24.942	25.007	24.995
±1000	99.963	99.570	99.698	99.481	99.719	99.959

Table 4-5: Normalized $CF_{B\text{-}1M}$

Step Load Change ΔP_L (MW) in Area A	Normalized $CF_{B\text{-}1M}$					5-minute-average
	1st minute	2nd minute	3rd minute	4th minute	5th minute	
±100	1.000	1.000	1.000	1.000	1.000	1.000
±500	25.006	24.997	24.988	25.016	24.964	25.010
±1000	100.049	99.969	99.895	99.963	99.631	100.086

Table 4-4 confirms that the ratio between normalized $CF_{A\text{-}1M}$ for a single-step-load-change in area A is equal to the square of the ratio between the corresponding magnitudes of the step load changes. Similarly Table 4-5 confirms that the ratio between normalized $CF_{B\text{-}1M}$ for a single-step-load-change in area A is equal to the square of the ratio between the corresponding magnitudes of the step load changes.

Therefore, if CF_{1M} for one single-step-load-change is known, CF_{1M} for any given single-step-load-change can be calculated using this quadratic relationship.

4.2 Significant period of CF_{1M} after a step-load-change

According to (3.2) and (3.3), CPS1 is calculated by averaging CF_{1M} values over a rolling 12-month-period. This involves summing the CF_{1M} values over the rolling 12-month-period. Magnitudes of CF_{1M} values subsequent to a single-step-load-change gradually reduce in each minute as the transients caused by the load change dies down. Therefore, CF_{1M} values few minutes after the single-step-load-change can be neglected in CPS1 calculation without introducing a significant error.

Table 4-6 and Table 4-7 tabulate the normalized CF_{1M} values for area A and area B respectively. Corresponding CF_{1M} value of the first minute of each single-step-load-change is taken as the base for normalization for each minute.

Table 4-6: Normalized $CF_{A\text{-}1M}$

Step Load Change ΔP_L (MW) area A	$(CF_{A\text{-}1M}/CF_{A\text{-}1M \text{ of first minute}})\times 100\%$				
	1st minute	2nd minute	3rd minute	4th minute	5th minute
±100	100.0000	0.6294	0.3222	0.0568	0.0048
±500	100.0000	0.6284	0.3218	0.0566	0.0048
±1000	100.0000	0.6270	0.3213	0.0565	0.0048

Table 4-7: Normalized $CF_{B\text{-}1M}$

Step Load Change ΔP_L (MW) area A	$(CF_{B\text{-}1M}/CF_{B\text{-}1M \text{ of first minute}})\times 100\%$				
	1st minute	2nd minute	3rd minute	4th minute	5th minute
±100	100.0000	-27.4758	-2.2371	-0.2329	-0.0346
±500	100.0000	-27.4656	-2.2355	-0.2329	-0.0346
±1000	100.0000	-27.4535	-2.2336	-0.2326	-0.0345

As illustrated in Table 4-6 and Table 4-7, the normalized CF_{1M}, diminishes rapidly as the time increases. Hence, the contribution to the average CF_{1M} from individual CF_{1M} values rapidly decreases as the time increases. In this example, after the 3rd minute, CF_{1M} becomes less than 0.3 % of the first minute CF_{1M}. After the 4th minute, it is less than 0.04 %. Hence in CPS1 calculations, it is sufficient to consider CF one-minute contributions of first two to three minutes subsequent to a single-step-load-change. Exact number of CF one-minute values required for CPS1 calculation depends on the targeted accuracy of CPS1 and on the rate at which the dynamics of the power system dies down.

4.3 Estimation of CF and its components in response to a multi-step-load-change

The rest of this chapter proposes three methods to estimate CF_{1M} for a multi-step-load-change based on the relationships established between Δf, ΔP, CF_{1M} and single-step-load-change in sections 4.1 and 4.2. The first method presented in section 4.3.1 is applicable when the magnitude of the step load changes and the exact time of the load changes are known. The second method presented in section 4.3.2 is applicable only when the magnitude of the step load changes and time span between consecutive load changes are known. The third method presented in section 4.3.3 is applicable when the probability distribution of the load change and the load sampling frequency are known.

4.3.1 Estimation of CF_{1M} for a multi-step-load-change, when the magnitude of the step load changes and the exact time of the load changes are known – Superposition Method

It was established in section 4.1.1 that $\Delta f^{\,i}$ and $\Delta P^{\,i}$ values for single-step-load-changes are proportional to the magnitude of the step load changes. It was also shown that Δf_{1M} and ΔP_{1M} values also to maintain the same relationship with the step load changes.

Any given multi-step-load-change could be split into a series of single-step-load-changes. Since the two-area system under consideration is modeled as a linear system, $\Delta f^{\,i}$ and $\Delta P^{\,i}$ for a multi-step-load-change could be obtained by superpositioning $\Delta f^{\,i}$ and $\Delta P^{\,i}$ corresponding to each single-step-load-change, provided that no system limits are reached. In order to obtain $\Delta f^{\,i}$ and $\Delta P^{\,i}$ corresponding to each step-load-change in the multi-step-load-change, recorded $\Delta f^{\,i}$ and $\Delta P^{\,i}$ waveforms must be suitably scaled using linear relationship between $\Delta f^{\,i}$, $\Delta P^{\,i}$ and the magnitude of the single-step-load-change. In superpositioning step-load-changes, it is important to maintain the chronological order of the load changes in the multi-step-load-change as well as the exact time of the load changes.

In order to validate the superpositioning method proposed above, a multi-step-load-change given in Figure 4-12 was applied to area A and area B. Figure 4-13 to Figure 4-15 show a comparison between the waveforms obtained from time domain simulation and superposition method.

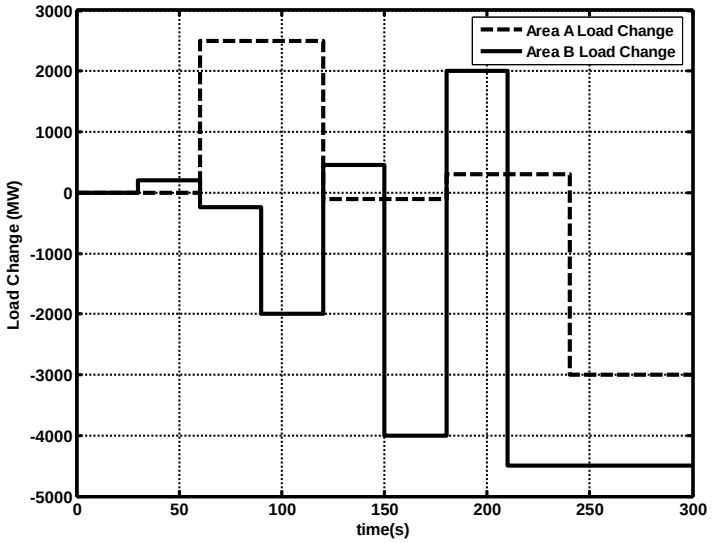

Figure 4-12: Multi-step-load-change in area A and area B

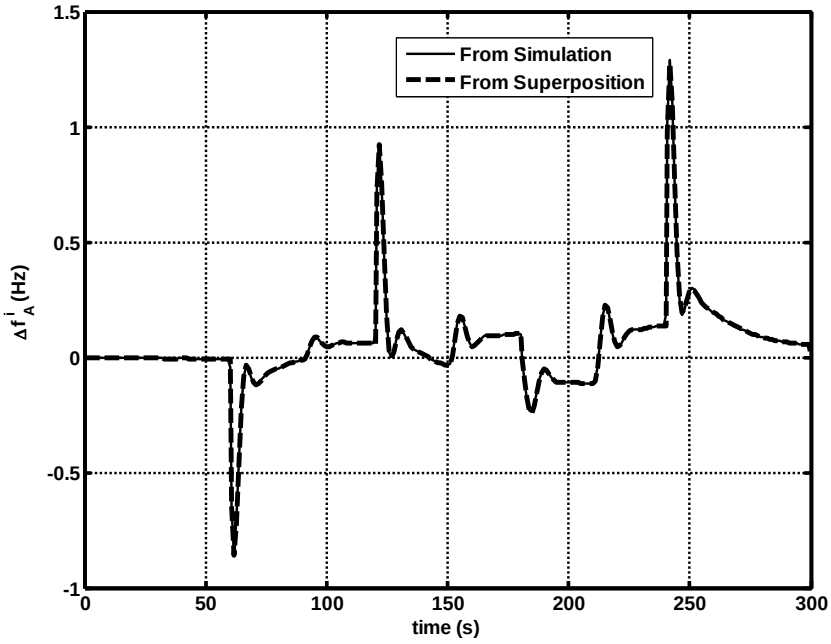

Figure 4-13: $\Delta f_A^{\,i}$ for a multi-step-load-change in area A and area B

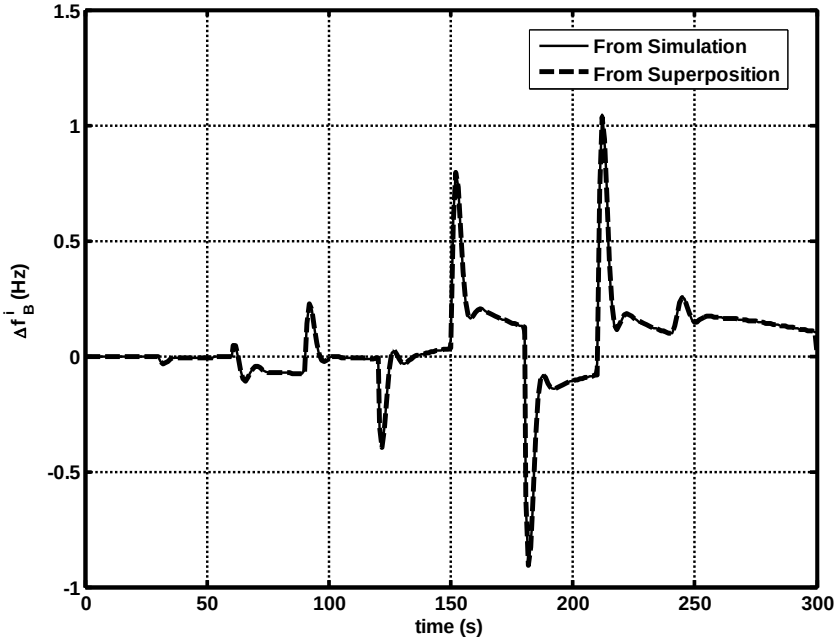

Figure 4-14: $\Delta f_B{}^i$ for a multi-step-load-change in area A and area B

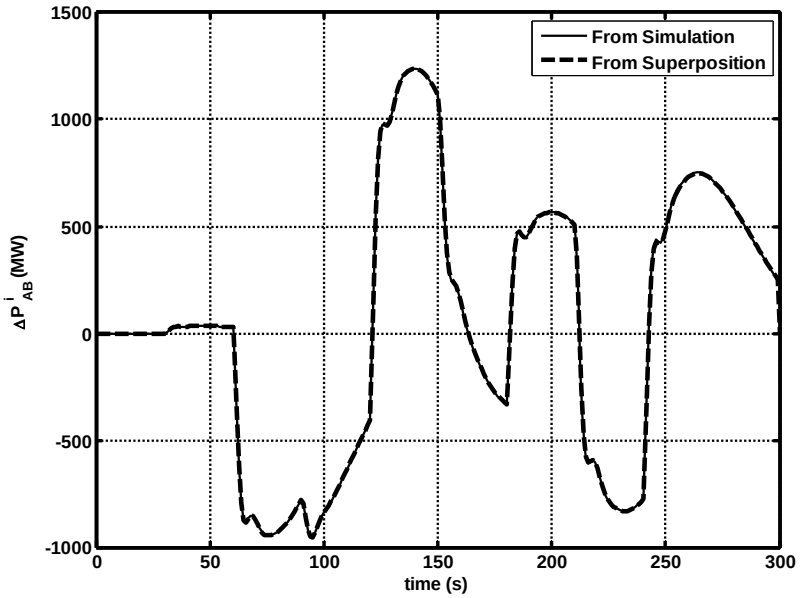

Figure 4-15: $\Delta P_{AB}{}^i$ for a multi-step-load-change in area A and Area B

Figure 4-13 to Figure 4-15 show a close match between plots obtained directly from simulation and from superposition. Hence, from the superposition method, Δf^i and ΔP^i for a multi-step-load-change could be constructed knowing the Δf^i and ΔP^i values for a single-step-load-change. Δf_{1M} and ΔP_{1M} for the multi-step-load-change could then be found by sampling the constructed Δf^i and ΔP^i profiles at each AGC cycle and then averaging them at the end of each minute. CF_{1M} values for the duration of load change could then be found by substituting these Δf_{1M} and ΔP_{1M} values in (3.7). Then, using (3.5) and (3.2), CPS1 for the duration of the load change could be found.

4.3.2 Estimation of CF_{1M} for a multi-step-load-change, when the magnitudes of the step-load-changes and time span between consecutive load changes are known – Approximate Method.

Following important observations were established in sections 4.1.2 and 4.2 respectively.

a. CF_{1M} values for single-step-load-changes are proportional to the square of the magnitudes of the corresponding load changes. The proportionality constant could be found if CF_{1M} values for a single-step-load-change is known.
b. CF_{1M} values for a single-step-load-change diminishes rapidly as the time increases. CF_{1M} values few minutes after the single-step-load-change is negligible compared to the CF_{1M} value of the first minute.

As mentioned in section 4.3.1, any given multi-step-load-change could be split into a series of single-step-load-changes. If the time span between two step-load-changes is sufficient so

that the CF_{1M} values due to previous load change is negligible when the second step-load-change is applied, CF_{1M} due to each step-load-change could be summed and averaged to get CF_{1M} of multi-step-load-change. CF_{1M} contribution due to each step-load- change could be calculated using the quadratic relationship between CF_{1M} and a single-step- load-change.

This method is demonstrated below where the average CF_{1M} values estimated using the above method for a simple multi-step-load-change is compared with the time domain simulation results. The multi-step-load-change is depicted in Figure 4-16, where the magnitude of the load increase or load decrease is marked with an arrow for a time period of 1080 seconds (i.e. 18 minutes). The arrow directing upwards depicts an increase in load with reference to the previous load change while the arrow directing downwards depicts a decrease in load with reference to the previous load change.

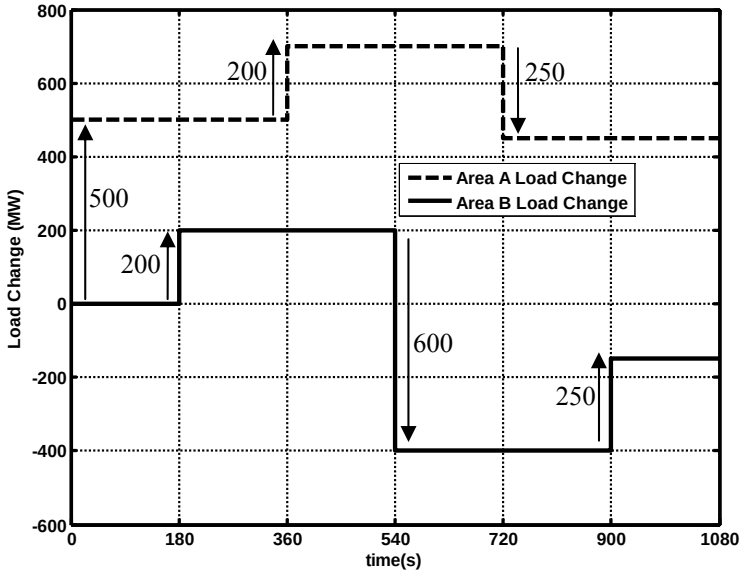

Figure 4-16: Multi-step-load-change

It was shown in section 4.2, for a two-area system, the CF_{1M} values beyond the third minute are negligible. Hence, in this example, it is assumed that the transients caused by each load change decays within 3 minutes (i.e. 180 seconds). Therefore, step-load-changes are applied alternatively in area A and B with 3 minutes' time span between every step change. In practice, load changes do not happen in steps. This necessitated the load curve for each area to be sampled at a constant time interval to obtain a step-load-curve. As the step-load-changes are applied alternatively in area A and B with 3 minutes' time span, each area load curve was sampled at 6 minute cycles (i.e. twice the time span between two consecutive step-load-changes in area A and area B) assuming that the load does not vary between any two sampling points.

In order to estimate the average CF_{1M} values for the multi-step-load-change given in Figure 4-16, CF_{1M} values for a 500 MW-step-load-change in area A and B are used. Table 4-8 shows CF_{1M} values for area A and B for a 500 MW single-step-load-change for the first 5 minutes. CF_{1M} values were calculated using (3.7). However those values were too small in magnitude, hence to increase the readability, each calculated value were divided by the square of the target frequency bound (ε^2) which is taken as 0.000324 Hz^2 (i.e. ε = 0.018 Hz, which is the value used for Eastern Interconnection of the North American electric grid [32]).

Table 4-8: CF_{1M} for a 500MW step-load-change in area A and area B

CF_{1M}	1st minute	2nd minute	3rd minute	4th minute	5th minute	Sum of CF_{1M} for first 3 minutes
±500MW-step-load-change in area A						
$CF_{A\text{-}1M}$	3.1784	0.0084	0.0071	0.0012	0.0001	**3.1939**
$CF_{B\text{-}1M}$	-0.4124	0.1058	0.0082	0.0009	0.0001	**-0.2984**
±500MW-step-load-change in area B						
$CF_{A\text{-}1M}$	-0.3845	0.0985	0.0077	0.0008	0.0001	**-0.2783**
$CF_{B\text{-}1M}$	1.2872	0.0508	0.0080	0.0010	0.0001	**1.3460**

CF_{1M} values for the first 3 minutes are highlighted in Table 4-8. The sum of these highlighted CF_{1M} values are shown in the last column of table with **bold text.** These values shown in bold text can be scaled based on the quadratic relationship between CF_{1M} and load change to get the sum of CF_{1M} for a single-step-load-change of a different magnitude. Table 4-9 tabulates sum of CF_{1M} values for the first 3 minutes for the multi-step-load-change in Figure 4-16.

Table 4-9: Sum of CF_{1M} values for the multi-step-load-change

Area A step-load-change			**Area B step-load-change**		
(MW)	**CF_{1M} contribution for first 3 minutes**		**(MW)**	**CF_{1M} contribution for first 3 minutes**	
	$CF_{A\text{-}1M}$	**$CF_{B\text{-}1M}$**		**$CF_{A\text{-}1M}$**	**$CF_{B\text{-}1M}$**
500	3.1939	-0.2984	200	-0.0445	0.2154
200	0.5110	-0.0477	-600	-0.4008	1.9382
-250	0.7985	-0.0746	250	-0.0696	0.3365
Total	**4.5034**	**-0.4207**		**-0.5149**	**2.4901**

The last row of Table 4-9 shows the total contribution to CF_{1M} from the load changes in area A and B. In this row, columns 2 and 3 show the contributions to CF_{1M} of area A and B from the load changes in area A. Similarly, columns 5 and 6 in the last row show the contributions to CF_{1M} of area A and B from load changes in area B.

Table 4-10 tabulates the CF_{1M} value for area A and B averaged over the 18-minute period. This way of estimating average CF_{1M} is referred to as the Approximate Method in Table 4-10 (and thereafter), as the transients beyond the 3rd minute are ignored. Here in calculating the average CF_{1M}, the summation of CF_{1M} values during the 18-minute period is divided by the number of minutes, as each CF_{1M} value was already divided by ε^2.

The same table also gives the average CF_{1M} values for area A and area B, for the multi-step-load-change, obtained by a Time Domain Simulation. Time domain simulation uses the multi-step-load-change and the two-area test system to estimate the average CF_{1M} value. This method is referred to as TD Simulation in Table 4-10 (and thereafter).

Table 4-10: Comparison of average CF_{1M} values

	Approximate method	**TD Simulation**	**% Error**
Average $CF_{A\text{-}1M}$	(4.5034-0.5149)/18 = 0.2216	0.2234	-0.81
Average $CF_{B\text{-}1M}$	(-0.4207+2.4901)/18 = 0.1150	0.1130	1.77

As shown in the last column of Table 4-10, the maximum percentage error of average CF_{1M} in the Approximated Method is less than 2 % when compared with the TD Simulation Method.

Table 4-11 gives the CPS1 values for area A and area B (denoted by $CPS1_A$ and $CPS1_B$ respectively), calculated using (3.2). The % error in the Approximate Method when

compared with the TD Simulation Method is shown in the last column of Table 4-11. The error in CPS1 is less than 0.2 % for the 18-minute period considered in the above example.

Table 4-11: Comparison of CPS1values

	Approximate method	**TD Simulation**	**% Error**
$CPS1_A$	177.84	177.66	0.101
$CPS1_B$	188.50	188.70	-0.106

Therefore, under the Approximate Method described above, CPS1 can be approximately estimated for a multi-step-load-change, given the area load data with the time span between consecutive load changes and the CF_{1M} values tabulated in Table 4-9.

4.3.3 Estimation of CF_{1M}, when the probability distribution of load change and load sampling frequency are known – PDF Method

Using load forecasting techniques, the load forecast for future operations could be obtained as a probability distribution of load for a particular period of time. A similar probability distribution with following features is assumed to be available to forecast the load change in each area of a two area system.

1. Load in a given area is a continuously changing function of time. In order to estimate the load change, the continuously changing load may be sampled at an interval of "*m"* minutes. Using these sampled load values, a multi step load curve could be constructed to approximate the continuously changing load. Here, 1/*m* is the load sampling frequency.
2. Load in area A and B are not sampled at the same instant of the time to avoid

interactions of transients caused by load change in area A and area B. It is clear that the optimal time separation between sampling instants for area A and area B is half of the sampling interval, that is, *m*/2 minutes.

In the absence of actual load change probability distribution, a zero mean *Normal Distribution* was assumed for area A and area B load change probability distributions. Standard deviation of each distribution was varied to obtain different area load change probability distributions. Figure 4-17 depicts the area load change probability density function for an area, where ΔP_L is the load change and $p(\Delta P_L)$ is the probability density for a load change of ΔP_L. In order to avoid unrealistic rates of load changes, the normal probability density function was modified by imposing upper and lower limits for a load change as shown in the Figure 4-17.

.

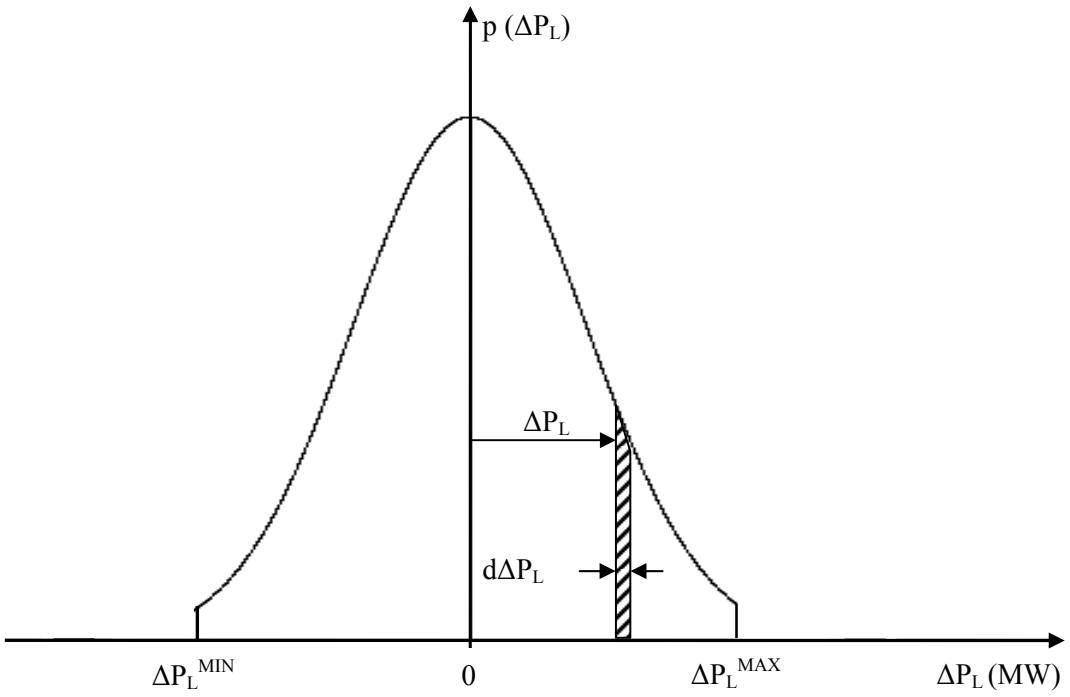

Figure 4-17: Area load change probability density function

In Figure 4-17, ΔP_L^{MIN} and ΔP_L^{MAX} are the maximum and minimum limits of ΔP_L, which were taken as $\Delta P_L^{MAX}=|\Delta P_L^{MIN}|$=2000 MW and 4000 MW for area A and B respectively. These limits were chosen to be equal to 10% of the nominal system load in each area.

The area load change probability density function shown in Figure 4-17 can be expressed as a probability density function given by (4.1).

$$p(\Delta P_L) = \frac{1}{\sqrt{2\pi}\sigma} e^{-\frac{1}{2}\left(\frac{\Delta P_L}{\sigma}\right)^2}, \quad \Delta P_L^{min} \le \Delta P_L \le \Delta P_L^{max} \tag{4.1}$$

where, σ is the standard deviation of the distribution.

In order to estimate the average CF_{1M} for the period of time represented by the area load change probability density function shown in Figure 4-17, consider the following information presented earlier in this chapter.

1. For a single-step-load change, CF_{1M} values after 3 minutes are negligible compared to CF_{1M} value of the first minute. Sum of CF_{1M} for the first 3 minutes are tabulated in Table 4-12.

Table 4-12: Sum of CF_{1M} values for the first 3 minutes for ± 500MW step-load-change

	Sum of CF_{1M}
Load-change in area A	
$CF_{A\text{-}1M}$	3.1939
$CF_{B\text{-}1M}$	-0.2984
Load-change in area B	
$CF_{A\text{-}1M}$	-0.2783
$CF_{B\text{-}1M}$	1.3460

2. Load change in area A and B were approximated by a multi-step-load-change. The time span between two consecutive steps in the same area was *m* minutes and time span between two consecutive steps in area A and B was *m*/2 minutes.

Using the "*Approximate Method"* presented in section 4.3.2, now, we could write the average CF_{1M} of area A, for step-load-changes of ΔP_{LA} in area A and ΔP_{LB} in area B, as shown in (4.2).

$$\begin{aligned} \text{Avg}\left(CF_{A\text{-}1M}\right) &= \frac{1}{m*N}\sum\left\{\left(\frac{\Delta P_{LA}}{500}\right)^2 *(3.1939)*n_A\right\} \\ &+ \frac{1}{m*N}\sum\left\{\left(\frac{\Delta P_{LB}}{500}\right)^2 *(-0.2783)*n_B\right\} \end{aligned} \tag{4.2}$$

where, n_A is the number of load changes in area A with magnitude ΔP_{LA} and n_B is the number of load changes in area B with magnitude ΔP_{LB}. N is the total number of step load changes in a given area.

In (4.2), ratio n_A/N represents the probability of ΔP_{LA} load change in area A. Similarly, ratio n_B/N represents the probability of ΔP_{LB} load change in area B. When N is large these probabilities could be expressed as follows.

$$\frac{n_A}{N} = p(\Delta P_{LA}) * d\Delta P_{LA}$$

$$\frac{n_B}{N} = p(\Delta P_{LB}) * d\Delta P_{LB}$$

where, $p(\Delta P_{LA})$ and $p(\Delta P_{LB})$ are the probability density functions of load changes in area A and area B respectively. $d\Delta P_{LA}$ and $d\Delta P_{LB}$ represent the width of a small bin as shown in Figure 4-17.

For very small $d\Delta P_{LA}$ (which implies large N) the function $p(\Delta P_{LA})$ is continuous and summation becomes the integration in finding the average $CF_{A\text{-}1M}$, which is given as ;

$$\begin{aligned} \text{Avg } CF_{A\text{-}1M} = & \frac{1}{m * \beta_A} \int \left\{ \left(\frac{\Delta P_{LA}}{500} \right)^2 * (3.1939) * p(\Delta P_{LA}) \right\} d\Delta P_{LA} \\ & + \frac{1}{m * \beta_B} \int \left\{ \left(\frac{\Delta P_{LB}}{500} \right)^2 * (-0.2783) * p(\Delta P_{LB}) \right\} d\Delta P_{LB} \end{aligned} \tag{4.3}$$

Similarly, the average $CF_{B\text{-}1M}$ could be written as given in (4.4).

$$\text{Avg } CF_{B\text{-}1M} = \frac{1}{m * \beta_{B}} \int \left\{ \left(\frac{\Delta P_{LB}}{500} \right)^2 * (1.3460) * P(\Delta P_{LB}) \right\} d(\Delta P_{LB}) + \frac{1}{m * \beta_{A}} \int \left\{ \left(\frac{\Delta P_{LA}}{500} \right)^2 * (-0.2984) * P(\Delta P_{LA}) \right\} d(\Delta P_{LA}) \quad (4.4)$$

where, $ß_A$ and $ß_B$ are the correction factors to account for the modification of the probability density function by limiting the range of load-change between ΔP_L^{MIN} and ΔP_L^{MAX}.

According to the above analysis, average CF_{1M} for area A and area B could be estimated using (4.3) and (4.4), given the area-load-change-distribution curve for each area. Then using (3.2), CPS1 could be found.

Chapter 5
Results and Discussion

Three methods of estimating average CF_{1M} were introduced in sections 4.3.1, 4.3.2 and 4.3.3 of Chapter 4. These three methods, which were referred to as "Superposition Method", "Approximate Method" and "PDF Method" respectively, could be used to estimate CPS1 without carrying out a TD Simulation.

In Superposition Method, estimation of Δf_{1M} and ΔP_{1M} values using the Δf and ΔP profiles (constructed using superposition) would have the same accuracy as time domain simulation values, if the system limits are not reached. However, similar to a TD Simulation, Superposition Method requires the exact time the load changes have occurred. Hence this method is not suitable to estimate CPS1 from the load change probability distribution and will not be discussed further in this thesis.

One of the major objectives of this thesis is to develop a simple method to estimate CPS1 from load change probability distribution. The PDF Method serves this purpose. Approximate Method sets an intermediate step between TD Simulation Method and PDF Method and it is useful to understand the approximation errors in the PDF Method

In this chapter, the accuracy of PDF Method with respect to TD simulations under wide range of conditions is examined and validity of the assumptions made in developing the PDF Method is investigated.

5.1 Validation of PDF method

In order to compare Approximate Method and PDF Method with TD Simulation method, load change probability density functions were assumed for area A and area B. Then, random load curves were generated for area A and area B. TD Simulation method used these load curves and the two area system model (presented in Chapter 3) to estimate CPS1. Approximate Method used load change magnitudes and time span between two consecutive load changes where as PDF method used the probability density functions and time span between consecutive load changes (or frequency of load change). In addition, both Approximate Method and PDF Method use four system constants tabulated in Table 4-12. Following case studies compare results from PDF Method and Approximate Method against TD Simulations for different conditions.

5.1.1 Case Study 1 – Comparison of load-change-distributions with different standard deviations

In order to investigate the performances of Approximate and PDF methods for various magnitudes of load changes, two load change distributions for each area were selected. In the first set of load change distributions, standard deviations of 300 and 600 for area A and B respectively were assumed. The second set of distributions assumed standard deviations of 600 and 1200 for area A and B respectively. Five thousand random step-load-changes were generated for each area distribution and it was assumed that the load in each area was sampled at intervals of 6 minutes (i.e. $m = 6$).

In generating random load patterns, load in area A and B were allowed to vary ± 25 % from their initial load levels of 20,000 MW and 40,000 MW for area A and B, respectively. That is, load in area A was allowed to vary between 15,000 MW to 25,000 MW and load in area B was allowed to vary between 30,000 MW to 50,000 MW. The lower and upper limits of load-change allowed for area A was ± 2000 MW where as it was ± 4000 MW for area B.

Table 5-1 tabulates average CF_{1M} values (denoted by avg CF_{1M}) calculated using TD Simulation Method, Approximate Method and PDF Method for the two sets of probability distributions.

Table 5-1: Comparison of average CF_{1M}

Area-load-change-distribution		Avg CF_{1M}	TD Simulation Method	Approximate Method	PDF Method	% Error Compared to TD Simulation Method	
σ_A	σ_B					Approximate Method	PDF Method
300	600	Area A	0.10752	0.11146	0.11308	3.7	5.2
		Area B	0.28296	0.28771	0.29611	1.7	4.6
600	1200	Area A	0.41747	0.42984	0.44768	3.0	7.2
		Area B	1.08420	1.10340	1.17220	1.8	8.1

According to Table 5-1, the error in Approximate Method is less than 3.7 % whereas the error in PDF Method is less than 8.1 %, when compared with TD Simulation Method.

Table 5-2 tabulates CPS1 values corresponding to the average CF_{1M} values tabulated in Table 5-1.

Table 5-2: Comparison of CPS1 values

Area-load-change-distribution		Area	CPS1 (%)			% Error		
σ_A	σ_B		TD Simulation Method (1)	Approximate Method (2)	PDF Method (3)	(1) with (2)	(1) with (3)	(2) with (3)
300	600	A	189.2	188.9	188.7	-0.4	-0.6	0.2
		B	171.7	171.2	170.4	-0.5	-1.3	0.8
600	1200	A	158.3	157.0	156.2	-1.2	-2.1	-0.8
		B	91.6	89.7	88.3	-1.9	-3.3	-1.4

Note that all three methods of estimating CPS1 have approximately matching CPS1 values. The maximum error of Approximate Method and PDF Method when compared with the TD Simulation Method is less than 1.9% and 3.3%, respectively.

There are two components in the error 1.9 % associated with the Approximated Method.

1. Error in neglecting CF_{1M} values 3 minutes after a step load-change: Although, CF_{1M} values 3 minutes after a step-load-change are not significant, compared to CF_{1M} values within the first 3 minutes, neglecting these small contributions to CF_{1M} causes a small error.
2. Variation of four constants tabulated in Table 4-12 with the system operating point: When the load in each area deviates from their nominal value, these constants also change slightly. Case Study 3 presented later in this section will address the properties of this component of error in detail.

The error between Approximate and PDF Methods is due to the finite sample size (5000 samples) of load-changes that was used in Approximate Method. In order to explain the error due to the sample size, consider histograms shown in Figure 5-1 and Figure 5-2. These histograms show the probability distribution of load-change for random load pattern generated using the probability distribution with standard deviations of 600 and 1200 for area A and area B, respectively. Width of individual bin in each of this histogram is 200 MW. Height of each bin in these histograms represents the probability of load-change that lies within each bin.

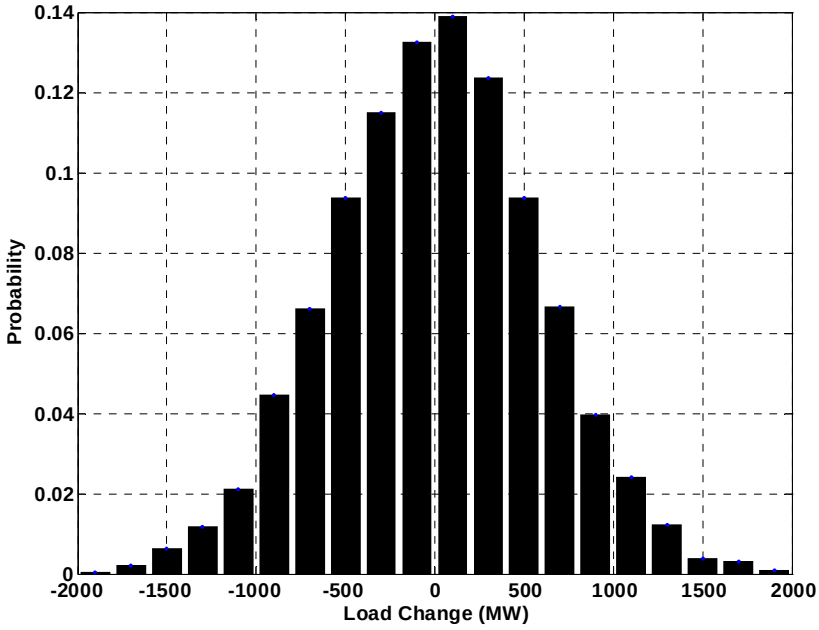

Figure 5-1: Load-change probability histogram of area A

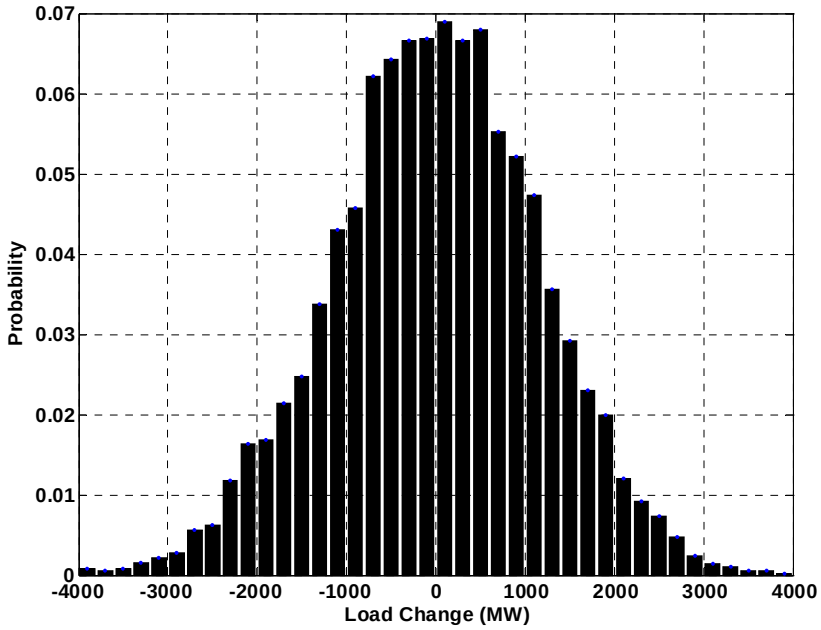

Figure 5-2: Area-load-change probability histogram of area B

Histograms shown in Figure 5-1 and Figure 5-2 represent the actual probability distributions of load-changes used in Approximate Method. It can be easily seen that these probability distributions are slightly different from the modified normal probability density function used in PDF Method. This deviation is a result of small 5000 load-change-samples used in the estimation. However, if there were enough load change samples, then the probability distribution shown in histograms and original probability distribution that was used to generate random load-changes will be the same. This would reduce the estimation error between Approximate Method and PDF Method. On the other hand, if an accurate probability distribution function is available to be used in PDF method, then the estimation error between the Approximate Method and the PDF Method will diminish.

Figure 5-3 depicts how CPS1 values estimated using Approximate Method reach towards the CPS1 values estimated using PDF Method when the numbers of load-change-samples are increased.

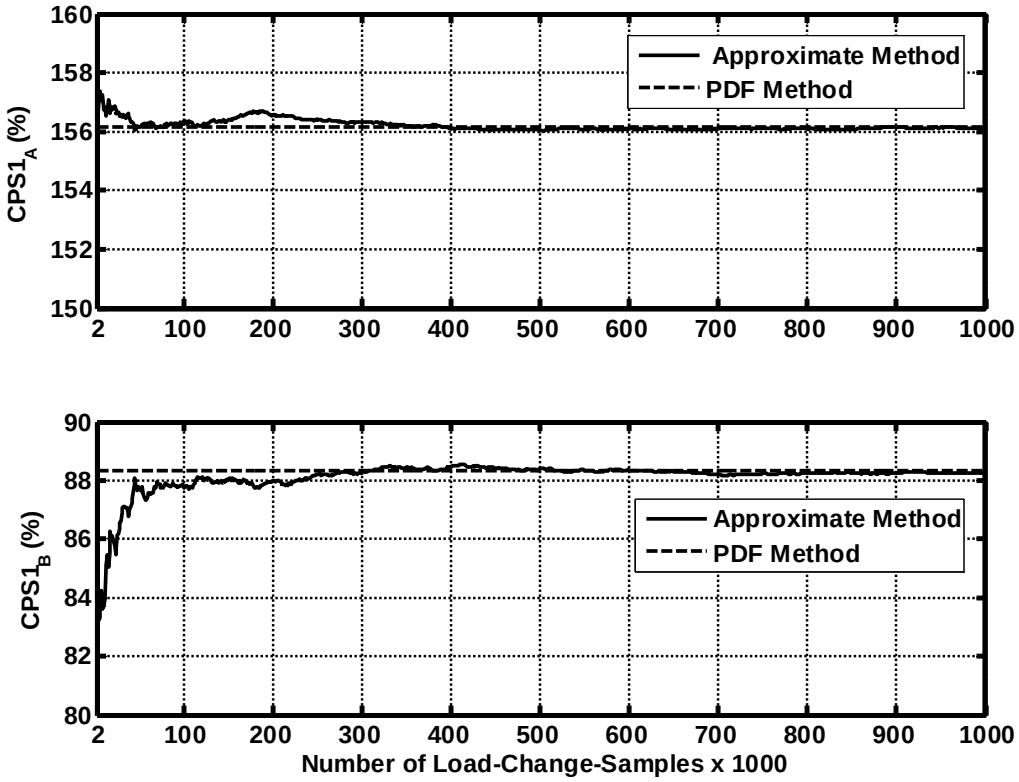

Figure 5-3: Comparison by varying the number of load-change-samples

In Figure 5-3, load-change-samples used in CPS1 calculations were varied between 2,000 and 100,000 for each of the areas A and B. CPS1 values of area A and area B were estimated using the Approximate Method by increasing the number of samples by 1000. CPS1 values for PDF method were calculated using the original probability density function that was used to generate above samples.

It is apparent from Figure 5-3, as the number of load-change-samples increases; the CPS1 values estimated from Approximate Method converge towards the CPS1 values estimated from PDF Method.

5.1.2 Case Study 2 – Comparison of load-change-distributions with different sampling frequencies

Load sampling frequency or the time span between two load changes, m, is an important parameter when applying either Approximate Method or PDF method. In case study 2, $m = 6$ was used. In case study 2, Approximate and PDF Methods are compared with TD simulation method for $m = 4$ and $m = 2$ minutes. It is also important to note that when m is varied, size of load changes also change proportionately. In this case study, this is achieved by changing the standard deviation of load-change probability used to generate random load-changes proportional to m. Table 5-3 tabulates CPS1 values corresponding to four sets of probability distributions with $m = 4$ and $m = 2$ minutes.

Table 5-3: Comparison of CPS1 values with different sampling frequencies

Area-load-change-distribution			Area	CPS1 (%)			% Error	
m	σ_A	σ_B		TD Simulation Method (1)	Approximate Method (2)	PDF Method (3)	(1) with (2)	(1) with (3)
4	200	400	A	192.6	192.4	192.5	-0.2	-0.2
			B	180.6	180.2	180.3	-0.4	-0.3
	400	800	A	172.8	171.9	169.8	-1.0	-3.0
			B	122.9	121.8	121.0	-1.1	-1.9
2	100	200	A	196.7	196.4	196.2	-0.3	-0.5
			B	190.6	190.5	190.1	-0.2	-0.5
	200	400	A	185.9	185.2	184.9	-0.7	-1.0
			B	161.6	161.0	160.5	-0.6	-1.0

In Table 5-3, the maximum error of Approximate Method and PDF Method when compared with the TD Simulation Method is less than 1.1% and 1.9%, respectively. Based on these comparisons of CPS1, it can be concluded that the time between consecutive sampling points could be reduced up to 2 minutes without causing significant increase in the estimation error for both Approximate and PDF Methods.

5.1.3 Case Study 3 – Variation of four constants with system operating conditions

In case study 3, impact of system operating conditions on the four constants used in Approximate and PDF Methods were investigated. Table 5-4 tabulates these four constants evaluated under different operating conditions obtained by scaling initial load and generation each area by a factor ranging between 70 % and 130 %.

Table 5-4: Constants for various operating conditions

Operating condition as a percentage of initial conditions	Percentage change	Constants			
		± 500MW step-load-change in area A		± 500MW step-load-change in area B	
		Constants of area A	Constants of area B	Constants of area A	Constants of area B
70	-30	3.7191	-0.2467	-0.2267	1.6818
80	-20	3.5236	-0.2745	-0.2538	1.5565
90	-10	3.3489	-0.2911	-0.2704	1.445
100	0	3.1939	-0.2984	-0.2783	1.346
110	10	3.0596	-0.3	-0.2809	1.2584
120	20	2.9403	-0.2966	-0.2786	1.1802
130	30	2.8233	-0.2906	-0.2729	1.1101

It is evident from Table 5-4, that the constants vary according to the operating point. Figure 5-4 and Figure 5-5, also shows these variations in graphical format. From Figure 5-4 and Figure 5-5, it can be observed that the constants exhibit a symmetrical behavior around the 0% change in operating point. Therefore, a random load-change consists of both load increases and load decreases around the initial operating conditions, should have a cancellation effect in the estimation error.

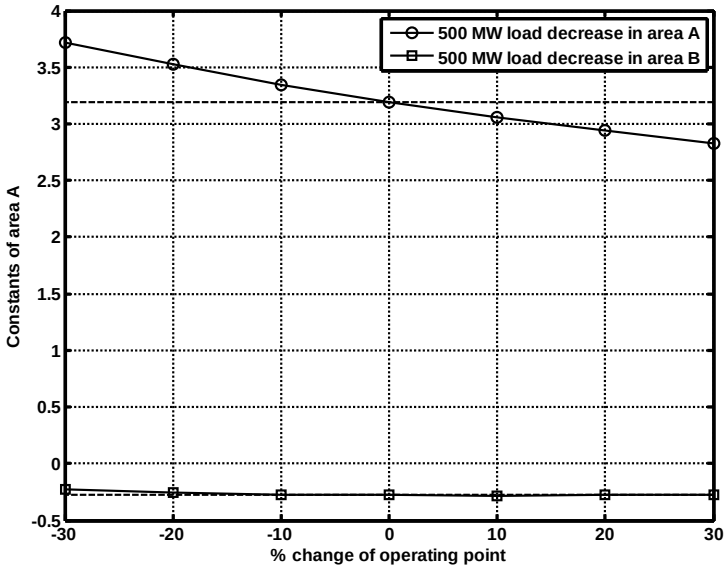

Figure 5-4: Constants of area A for different operating points

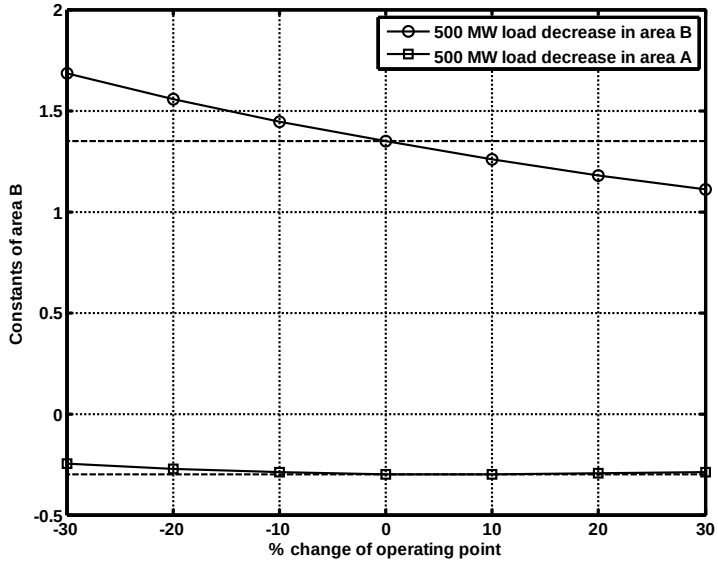

Figure 5-5: Constants of area B for different operating points

In order to validate the above argument, two sets of load distributions were assumed. In the first sets of distributions, the loads in area A and area B were varied up to ± 25% of the initial load conditions. In the second two distributions, the loads in area A and area B were varied up to ± 50% of the initial load conditions. All distributions assumed standard deviations of 300 and 600 for area A and B respectively. A sampling interval of 2 minutes is assumed in random load generation. The load conditions and CPS1 values of each distribution are shown in Table 5-5.

Table 5-5: Comparison of CPS1 values with different load conditions

Area	% Change	Minimum Load (MW)	Maximum Load (MW)	CPS1 (%)			% Error	
				TD Simulation Method (1)	Approximate Method (2)	PDF Method (3)	(1) with (2)	(1) with (3)
A	± 25%	15,000	25,000	167.7	166.6	166.1	-1.1	-1.7
B		30,000	50,000	111.3	110.5	111.2	-0.8	-0.1
A	± 50%	10,000	30,000	167.1	165.3	166.1	-1.8	-1.0
B		20,000	60,000	111.7	109.6	111.2	-2.1	-0.5

The maximum error of Approximate Method and PDF Method when compared with the TD Simulation Method is less than 2.1% and 1.7% respectively. Hence it can be seen that the error introduced by varying the load conditions by ± 50% is negligible and there is no significant impact on CPS1 by assuming same constant for wide range of operating conditions.

Chapter 6
Conclusion

The main contribution of this thesis is the development of a novel method to approximately estimate CPS1 for a two-area power system using the probability distribution of load change. The thesis also analyzed how well CPS1 evaluates the performance of a control area with respect to control of frequency and tie-line power flows.

In Chapter 3 it was shown that CPS1 is a linear function of CF, which is the base quantity used in calculating CPS1. CF was then de-composed into two terms, where each term provided an indication of how well a control area has met its control obligations. Term 1, which is proportional to a ratio between the square of frequency error (Δf) and square of targeted frequency error, is a measure of how well a control area controls its frequency with respect to targeted frequency. Term 2, which is proportional to the product of frequency error and tie-line power flow error (ΔP), is a measure of the support received from or given to adjacent control area. Based on the range of values that these two terms could take, it was shown that a control area is assured to be in compliance with NERC CPS1 standard, if it fulfills both its obligations of controlling frequency and tie-line power flows. Thus, it could be concluded that CPS1 correctly evaluates the control area performance.

In Chapter 4, three methods of estimating CPS1, without carrying out a time domain simulation, were developed. These methods were: Superposition Method, Approximate Method and PDF Method. All three methods were developed under the assumption that the actual load could be approximated by multi-step-load that could be obtained by sampling the

actual load curve. At the beginning of the chapter, two important relationships between Δf, ΔP and CF with the magnitude of a single-step-load-change were established. The first relationship showed that one-minute average values of Δf and ΔP were linearly proportional to the magnitude of the step-load-changes. The second relationship showed that the one minute CF values were proportional to the square of the magnitude of the step-load-changes. Further, it was shown that there are four constants for a given two-area system, which relates square of the load change to CF in each area. Therefore, magnitude of these constants determines how sensitive CF is for a given load-change.

Out of the three methods, Superposition method could be used to estimate CPS1 for a multi-step-load-change, when load change time information is available. This method uses the linear relationship between Δf, ΔP and a single-step-load-change. By recording the waveforms of Δf and ΔP for a single step-load-change, the same profiles for a multi-step-load-change could be constructed, which could then be used to calculate CF and then CPS1. This method is faster than time-domain simulation method and will yield accurate results as long as the limits of the system are not reached.

Approximate Method could be used to estimate CPS1, when the magnitudes of the step-load-changes and the time span between consecutive load changes are known. This method was then further expanded to estimate CPS1 given the probability distribution of the load change and the load sampling frequency.

In chapter 5, the Approximate Method and the PDF Method were validated against time domain simulation method. It was shown that the methods are reliable and CPS1 could be approximated with 5% accuracy.

Future Work

The simplified interconnected power system model used in this study represents only the minimum yet sufficient details required for a frequency control performance analysis. This simplification has the advantage of computational simplicity over detailed models. Further studies are required to develop a methodology to estimate parameters for the simplified interconnected power system model using available power system data.

Appendix A

When there is an imbalance between the torques acting on the rotor, the net torque causing acceleration (or deceleration) is given by,

$$T_a = T_m - T_e \tag{1}$$

$T_a =$ accelerating torque in Nm

$T_m =$ mechanical torque in Nm

$T_e =$ electrical torque in Nm

If J is the combined moment of inertia of the generator and turbine in kg.m^2, from laws of rotation, we have

$$J\frac{d^2\theta_m}{dt^2} = T_a = T_m - T_e \tag{2}$$

where θ_m is the angular displacement of the rotor with respect to the stationary reference axis on the stator. Since we are interested in the rotor speed relative to synchronous speed, the angular reference is chosen relative to a synchronously rotating reference frame moving with constant angular velocity, ω_{sm} in mechanical radians per second. That is,

$$\theta_m = \omega_{sm}t + \delta_m \tag{3}$$

where δ_m is the rotor position before disturbance at time, t=0, measured from the synchronously rotating reference frame. Derivative of (3) gives the rotor angular velocity, ω_m

$$\omega_m = \frac{d\theta_m}{dt} = \omega_{sm} + \frac{d\delta_m}{dt} \tag{4}$$

and the rotor acceleration is

$$\frac{d\omega_m}{dt} = \frac{d^2\theta_m}{dt^2} = \frac{d^2\delta_m}{dt^2} \tag{5}$$

Substituting (5) in (2), we have,

$$J\frac{d\omega_m}{dt} = T_a = T_m - T_e \tag{6}$$

The above equation (6) can be normalized, in terms of per unit inertia constant H, defined as,

$$H = \frac{\text{kinetic energy in watt-seconds at rated speed}}{\text{machine rating (or the VA base)}}$$

$$H = \frac{1}{2}\frac{J\omega_{0m}^2}{VA_{base}} \tag{7}$$

The moment of inertia J in terms of H is,

$$J = \frac{2H}{\omega_{0m}^2}VA_{base} \tag{8}$$

Substituting (8) in (6) gives,

$$\frac{2H}{\omega_{0m}^2}VA_{base}\frac{d\omega_m}{dt} = T_a = T_m - T_e \tag{9}$$

Rearranging yields,

$$2H\frac{d}{dt}\left(\frac{\omega_m}{\omega_{0m}}\right) = \frac{T_m - T_e}{\left(\frac{VA_{base}}{\omega_{0m}}\right)} \tag{10}$$

In (10), $T_{base} = \frac{VA_{base}}{\omega_{0m}}$, the equation of motion in per unit is,

$$2H \frac{d\omega_{r(pu)}}{dt} = T_{m(pu)} - T_{e(pu)} \tag{11}$$

where, $\omega_{r(pu)} = \frac{\omega_m}{\omega_{0m}} = \frac{\omega_r}{\omega_0}$ and ω_r is the angular velocity of the rotor in electrical radians/second and ω_0 is its rated value.

Equation (11) gives the relationship between rotor speed as a function of the electrical torque and mechanical torque. It can be represented in transfer function form as,

$$2H \times s\omega_{r(pu)} = T_{m(pu)} - T_{e(pu)} \tag{12}$$

where s is the Laplace operator. Above transfer function is illustrated in Figure A-1.

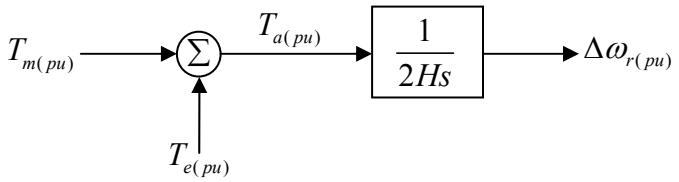

Figure A-1: Transfer function relating speed and torques

where,

s : Laplace Operator
T_m : Mechanical torque in pu
T_e : Electrical torque in pu
T_a : Accelerating torque in pu
H:Inertia constant in W-second/VA
$\Delta\omega_r$: Rotor Speed Deviation in pu

The relationship between power P and Torque T is given by,

$$P = \omega_r T \tag{13}$$

Now let us consider a small deviation Δ, from initial values which are denoted by subscript $_0$.

$$\left.\begin{aligned} P &= P_0 + \Delta P \\ T &= T_0 + \Delta T \\ \omega_r &= \omega_0 + \Delta\omega_r \end{aligned}\right\} \tag{14}$$

Substituting (14) in (13) we get,

$$P_0 + \Delta P = (\omega_0 + \Delta\omega_r)(T_0 + \Delta T) \tag{15}$$

By expanding (15),

$$P_0 + \Delta P = \omega_0 T_0 + \omega_0 \Delta T + \Delta\omega_r T_0 + \Delta\omega_r \Delta T \tag{16}$$

Since $P_0 = \omega_0 T_0$ and neglecting higher order terms in (16),

$$\Delta P = \omega_0 \Delta T + \Delta\omega_r T_0 \tag{17}$$

Hence,

$$\Delta P_m - \Delta P_e = \omega_0(\Delta T_m - \Delta T_e) + \Delta\omega_r(T_{m0} - T_{e0}) \tag{18}$$

At steady state,

$$T_{m0} = T_{e0} \text{ and } \omega_0 = 1 \text{ pu}$$

Hence

$$\Delta P_m - \Delta P_e = \Delta T_m - \Delta T_e \tag{19}$$

Figure A-1 can now be expressed in terms of power as illustrated in Figure A-2.

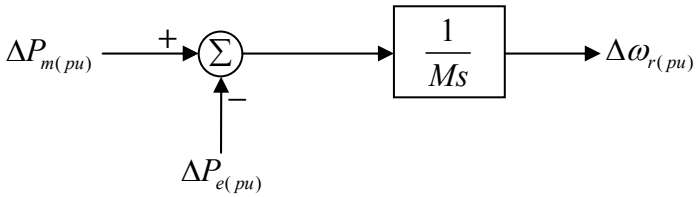

where $M = 2H$

Figure A-2: Transfer function relating speed and power

Appendix B

Types of Turbines

Steam Turbines

Steam turbines may be of either reheat type or non-reheat type. A steam turbine with a high pressure turbine can be modeled as a simple first order time lag as shown in Figure B-1.

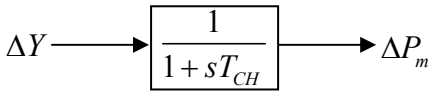

$T_{CH} = 0.3$ s (Typical value)

Figure B-1: Non-reheat steam turbine transfer function

Similarly the transfer function of a reheat steam turbine is given in Figure B-2.

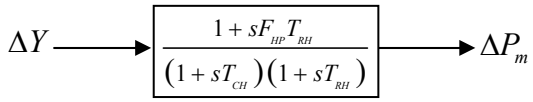

Typical Values:

$$F_{HP} = 0.3s \quad T_{RH} = 7.0s \quad T_{CH} = 0.3s$$

Figure B-2: Reheat steam turbine transfer function

Hydraulic Turbines

The block diagram of a generating unit with a hydraulic turbine is shown in Figure B-3. The governor of hydraulic units consists of a transient droop (R_T) in addition to the permanent droop (R_p). When the gate of the hydro turbine is opened, the output of the turbine decreases initially due to the high inertia of water. Then the output starts to increase to the desired level. Hence hydro turbine governors are designed to have relatively large transient droop, with long resetting times (T_R).

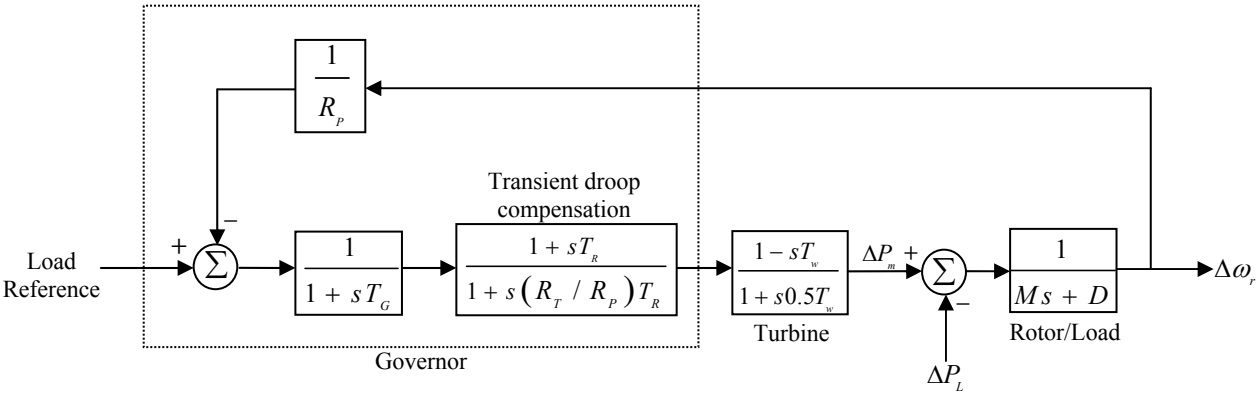

Typical values:

$T_w = 1.0s$ $R_P = 0.05$ $R_T = 0.38$ $T_G = 0.2s$ $M = 6.0s$ $T_R = 5.0s$ $D = 1.0$

Figure B-3: Block diagram of a hydraulic unit

References

[1] B.J. Kirby, J. Dyer, C. Martinez, R. A. Shoureshi, R. Guttromson, J. Dagle, "Frequency Control concerns in the North American Electric Power System," Oak Ridge National Lab., Oak Ridge, ORNL/TM-2003/41, 2002

[2] H.M. Dimond, G.S. Lunge, "Continuous Load-Frequency Control for Interconnected Power Systems," *AIEE Trans*, vol.67, pp.1483-1490, 1948

[3] Stan Mark Kaplan. (2009, April 14). *Electric Power Transmission: Background and Policy Issues*. Congressional Research Services, U. S. Department of State. Available: http://fpc.state.gov/documents/organization/122949. pdf

[4] NERC. *Technical Report.* (1992, July). *Control Area Concepts and obligations.* Available: http://www.nerc.com/docs/ docs /pubs/Control-Area-Concepts-and-obligations. pdf

[5] "Definitions of terminology for Automatic Generation Control on electric Power Systems," *IEEE Pub.*, no.94, Nov. 1965

[6] NERC. *Corporate website.* http://www.nerc.com

[7] M. Yao, R. R. Shoults, and R. Kelm, "AGC logic based on NERC's new Control Performance Standard and Disturbance Control Standard," *IEEE Trans. Power Syst.*, vol.15, No.2, May 2000

[8] NERC. *Glossary of Terms used in Reliability Standards*. (2008, February 12). [Online]. Available: http://www.nerc.com/files/Glossary_12Feb08.pdf

[9] N.Jaleeli and L.S.VanSlyck, “NERC’s new control performance Standards,” *IEEE Trans. Power Syst.*, vol.14, pp.1092-1099, Aug.1999

[10] Control Criteria Task Force, Performance Subcommittee, NERC, *Control Performance Standard and Disturbance Control Standard frequently asked questions*, Nov. 1996

[11] Tetsuo Sasaki and Kazuhiro Enomoto, “Statistical and Dynamic Analysis of Generation Control Performance Standards,” *IEEE Trans. Power Syst.*, vol. 17, No.2, May 2002

[12] P. Kundur, “Power System Stability and Control,” New York: McGraw-Hill, Inc, 1994, pp. 1-16, 581-626

[13] O.I. Elgerd, “Electric Energy Systems Theory,” New York: McGraw-Hill, 1971

[14] C.K. Duff, “Control of Load, Frequency and Time of Interconnected Systems”, *AIEE Trans*, vol.64, pp.778-786, 1945

[15] A.J. Wood and B.F. Wollenberg, “ Power Generation, Operation and Control,” John Wiley and sons, 1984

[16] L.K. Kirchmayer, “Economic Control of Interconnected Systems,” New York, Wiley, 1959

[17] O. I. Elgerd and C.E. Fosha, "The megawatt-frequency control problem: A new approach via optimal control theory," *IEEE Trans. Power APP. and Syst.*, vol. PAS-89, No.4, 1970

[18] O. I. Elgerd and C.E. Fosha, "Optimum megawatt-frequency control of multi-area electric energy systems," *IEEE Trans. Power Apparatus and Syst.*, vol. PAS-89, pp. 556-563, 1970

[19] C. Concordia, L.K. Kirchmayer, E. A. Szymanski, "Effect of Speed-Governor Dead Band on Tie-Line Power and Frequency Control Performance, *AIEE Trans*, vol.76, part III, pp 429-434, 1957

[20] N. Jaleeli, D.N. Ewart, L.H. Fink, "Understanding Automatic Generation Control," *IEEE Trans. Power Syst.*, vol. 7, no. 3, pp. 1106-1122, Aug. 1992

[21] C. Concordia, S. B. Crary, E. E. Parker, " Effect of prime mover speed governor characteristics on power system frequency variations and tie-line power swings," *AIEE Trans*, vol.60, pp 559-567, 1941

[22] C. Concordia, L.K. Kirchmayer, "Tie-Line Power and Frequency Control of Electric Power Systems," *AIEE Trans*, vol.72, part III, pp 562-671, 1948

[23] Y.G. Rebours, D.S. Kirschen, M. Trotignon and S. Rossignol, "A survey of Frequency and Voltage Control Ancillary Services-Part1: Technical Features," *IEEE Trans. Power Systems*, vol. 22, no.1, Feb. 2007

[24] R.L. King, M.L. Ngo, R. Luck, "Interconnected system frequency response," *Proceedings of the Twenty-Eighth Southeastern Symposium,* pp 306-310, 1996

[25] N. Cohn, "Some aspects of tie-line bias control on interconnected power systems," *AIEE Trans. Power Apparatus and Systems*, vol. 75, pp. 1956

[26] N. Jaleeli, L.S. VanSlyck, "Tie-Line Bias Prioritized Energy Control," *IEEE Trans. Power Systems*, Vol. 10, No. 1, Feb. 1995

[27] N. Cohn, “Control of generation and power flow on Interconnected Systems,” New York, Wiley, 1971

[28] N. Cohn, “Considerations in the Regulation of Interconnected Areas,” *IEEE Trans. Power Apparatus and Systems*, vol. PAS-86, pp. 1527-1538, 1967

[29] B. Oni, H. Graham, L. Walker, “Investigation of non-linear Tie-Line Bias Control of Interconnected Power Systems,” *IEEE Trans. Power Apparatus Syst.*, vol.PAS-100, pp.2350-2356

[30] R.L. King, M.L. Ngo, R. Luck, “Implications of frequency bias settings on AGC,” *Proceedings of the Twenty-Seventh Southeastern Symposium,* pp 83-86, 1995

[31] *Performance Standard Reference Document*, version 3 (Accepted by NERC Resources Subcommittee on October 23, 2007)

[32] N. Jaleeli and L.S. VanSlyck, Principal Investigators, “Control Performance Standards and procedures for Interconnected Operation,” EPRI TR-107813, Apr. 1997